Modelling and Optimization of an Off-Grid Hybrid Power System for

Supplying Unmanned Offshore Installations in Eastern Malaysia

by

Moustafa Ahmed Moustafa Mansour

15816

Dissertation submitted in partial fulfillment of

the requirements for the

Bachelor of Engineering (Hons)

(Electrical and Electronics)

JANUARY 2015

Universiti Teknologi PETRONAS

Bandar Seri Iskandar

32610 Tronoh

Perak Darul Ridzuan

CERTIFICATION OF APPROVAL

Modelling and Optimization of an Off-grid Hybrid Power System for Supplying

Unmanned Offshore Installations in Eastern Malaysia

by

Moustafa Ahmed Moustafa Mansour

15816

A project dissertation submitted to the

Electrical & Electronics Engineering Programme

Universiti Teknologi PETRONAS

in partial fulfilment of the requirement for the

BACHELOR OF ENGINEERING (Hons)

(ELECTRICAL AND ELETRONICS)

Approved by,

_____

(Ir Mohd Faris bin Abdullah)

UNIVERSITI TEKNOLOGI PETRONAS

TRONOH, PERAK

January 2015

CERTIFICATION OF ORIGINALITY

This is to certify that I am responsible for the work submitted in this project, that the original work is my own except as specified in the references and acknowledgements, and that the original work contained herein have not been undertaken or done by unspecified sources or persons.

_____

Moustafa Ahmed Moustafa Mansour

ABSTRACT

In this project, investigation about the potential utilization of hybrid power system in the Malaysian offshore environment is examined. An unmanned offshore installation was selected for the study. The solar and wind energy potentials in Malaysia were investigated and the feasibility study of the project was proved by using meteorological data from the project location at Southeast China Sea. In addition to that, the installation power demand was estimated based on the load profile from Cutter Platform, World first unmanned offshore platform to be operated totally by renewable energy in the North Sea. Moreover, a hybrid power system topology was proposed to supply the loads on-board the offshore installation. Likewise, modelling and simulation of the hybrid power system was achieved using Matlab/Simulink environment. Finally, the optimization study was implemented to achieve the optimum design for the hybrid power system taking the cost reduction as the main objective function for the study. The results showed a great potential towards utilizing hybrid power systems in the Malaysian environment considering the highly solar irradiation levels in Malaysia. Also, the optimization study concluded that fuel consumption and fuel price are the most crucial parts in determining the cost effectiveness of a hybrid power system.

ACKNOWLEDGEMENT

With all the unexplored challenges waiting for me prior to the completion of my final year project, I am forever thankful to my beloved parents, who have given me the never-ending support to ensure that I have the courage and perseverance to go through difficulties and obstacles. I would like to dedicate this bachelor thesis to my much-loved parents my father and my mother who have been the source of motivation, passion, and greatness in my life.

My upmost gratitude is also addressed to those people who have helped me during the project. These include, generally, the staff of Electrical and Electronics Engineering department at Petronas University of Technology (UTP) for their kindness support and guidance during the project.

I would like to express a million thanks to my dearest Supervisor, Ir. Mohd Faris bin Abdullah for dedicating his time and effort towards the success of my final year project. His guidance, specifically, includes the completion of this project report.

Without all of the names I have stated above, final year project (FYP) report would not be completed with full satisfaction and on time.

TABLE OF CONTENTS

LIST OF FIGURES

LIST OF TABLES

CHAPTER 1 : INTRODUCTION

1.1   Project Background

In Malaysia, oil and gas industry has proven to be one of the most successful and emerging industries and the main pillar for Malaysia economic growth during the last twenty five years. The exploration and drilling operations have extended not only on the onshore scope but also on the offshore scope as well. The higher demand for energy to serve the uprising economy in Malaysia as well as other Southeast Asian countries has opened numerous opportunities for investments in the oil and gas industry.

The offshore explorations in Malaysia resulted in a promising future for the oil and gas reserves in Malaysia especially in the eastern part of Malaysia where all the major offshore operations take place. Initially, the offshore operation depended mainly on human workforce to operate, maintain, and monitor the process flow. Therefore, the cost for offshore operation increased rapidly due to the total dependence on manned installations.

Unmanned offshore installations have been implemented in the early 1980 in the offshore environment to reduce the operation and maintenance costs. In addition to that, unmanned installations were designed to operate effectively and precisely without the human interference which only exist to monitor and check the operation statistics. Supplying the unmanned installations with a reliable power source represented a huge challenge for the industry. Non-conventional power sources such as diesel generators and gas turbines are mainly used for supplying different loads and instrumentation devices.

However, during the unfavorable climatic conditions such as storms, monsoon, the generators and gas turbines showed a poor performance and have caused a regular power shortage on the electrical systems in the unmanned installations. Moreover, the climatic conditions in the offshore environment during the monsoon and stormy times usually obstruct the maintenance teams from fixing the occurred faults in the required time. Hence, the process could shut down for days till the process flow is restored completely.

Hybrid systems were introduced in the new era as an effective solution to provide off-grid and remote areas with clean and cheap power supply. A hybrid system is usually composed of two or three different conventional power sources such as solar energy

and wind energy. The development of technology has resulted in better performance and efficiency for the hybrid systems especially after introducing power converters, advanced (PV) systems and micro-wind turbines. Hybrid systems are being implemented nowadays to serve remote residential villages, off-grid small industrial areas and off-grid offshore installations which do not require an excessive generation capability.

1.2   Problem Statement

The unmanned installations represent a promising and cost effective future for the oil and gas offshore operations not only in Malaysia but also all over the world. Remote monitoring is the main key issue in the operation of unmanned offshore installations. Constant and persistent monitoring requires that the power system should be efficient, well-designed, commissioned according to the international standards and capable of operating in an immense and different range of conditions. Supplying unmanned installations with a reliable and well-founded power system will improve the process flow. Moreover, an efficient power system will reduce and minimize the faults and malfunctions occur as a result of the main dependence of the non-conventional power sources. Besides, implementing a power system which have conventional and non-conventional sources will maximize the reliability and performance of the system regardless of the poor maintenance or the unpredictable climatic conditions.

1.3   Objectives

- To conduct a theoretical and literature study about micro-grid hybrid power system in the offshore environment.
- To propose a design of an offshore micro-grid power system based on the theoretical studies.
- To model and simulate the power system components in order to obtain input data to the optimization model.
- To optimize the components of the power system based on the objective function of minimizing the cost of the power system components through the lifespan of the system.

1.4   Scope of Study

The project scope of study is to conduct a literature study about unmanned offshore installations. Then, the project feasibility will be examined using the meteorological data of the project location. After that, hybrid power systems will be analyzed and studied. Also, previous and ongoing research studies about implementing hybrid systems with conventional and non-conventional power sources will be reviewed. Then, analysis, modelling, simulation and optimization of the project will be carried out in order to achieve the study objectives. Finally, the optimization study will be implemented to achieve the optimum design for the hybrid system by using a cost effectiveness approach.

CHAPTER 2 : LITERATURE REVIEW

2.1 Oil and Gas Development in Malaysia

Malaysia is in the middle of a rapid economic growth started on 1980 and is expected to reach its peak on 2020 when Malaysia become a fully industrialized country. Oil and gas industry in Malaysia plays an important role in the country economy. The country has enormous energy resources with sufficient amounts such as the recoverable hydrocarbons reserves which estimated at 4.5 billion barrels of oil and 68 TCF of natural gas. Throughout the past century, the country mainly relied on four main energy sources (oil, natural gas, hydropower and coal), with an increasing dependence on oil and natural gas reserves [1].

The first commercial oil and gas development in Malaysia dated back to 1910 when the Sarawak Shell company (formed by Anglo-Saxon Petroleum Company) developed the Miri oil field in Sarawak. Starting with an 83 barrels per day 83 years ago, the oil and gas industry in Malaysia has emerged toward endless possibilities and opportunities and has grown to be a multi-billion dollar industry. The industry underwent a dramatic expansion with rapid intensification in exploration and development [2].

The majority of Malaysia recoverable hydrocarbon resources are located in the offshore part of Malaysia. Offshore oil field development requires special consideration during the exploration, appraisal, field development, and project implementation and field production phases. The scope of work and capital expenditure is generally greater for an offshore field development [2].

The development cost for offshore oil fields using all manned installations require a capital investment of millions of dollars. Moreover, the operation and maintenance costs will be much higher due to the existence of human factor. By comparison, the use of unmanned offshore installations would save a lot of resources, capital investments, and will reduce the operation and maintenance costs [3].

Based on a previous research study carried out by ESSO Malaysia for one of the company offshore fields Guntong A, the field development with all manned installation would have required a capital investment of US$440 million, an annual operating costs of US$27 million, and a total number of 224 personnel for operation and maintenance purposes. By comparison with the utilization of unmanned

installations, the capital investment cost for the development of the offshore field while using unmanned installations would have been about US$300 million, US$20 million for the annual operating costs, and a crew of 124 personnel for operation and maintenance purposes [3].

Unmanned offshore installations can provide economic benefits and savings for the development of offshore oil and gas fields. The use of the unmanned installations has resulted in significant reduction in capital investments and in annual operation and maintenance costs. The early generations of unmanned offshore installations provided operating experience and paved the way towards development and improvement in the new designs for unmanned installations. The performance of the newer generations have been highly accurate, precise and satisfactory. In addition to that, the older generations are being regularly upgraded through improvement programs [3].

To provide a sufficient power supply to the unmanned platforms, the older generations of unmanned platforms mainly used conventional power sources. The conventional power sources such as diesel and natural gas turbines used to supply the instrumentation and electrical devices with continuous power supply. However, the regular maintenance conventional power systems resulted in increasing the operating costs over the long term. In addition to that, during the monsoon time and the heavy rain season, the conventional systems failed to meet the requirements due to the sudden breakdown of the power sources [4].

The hybrid power system was introduced to overcome the unreliability and shortage capability for conventional power sources. The hybrid system is mainly implemented to supply the instrumentation loads which usually use a DC power source. The mixed hybrid system uses renewable sources of energy in line with the conventional power source. With a battery storage mechanism and intelligent controlling and monitoring of the conventional power source fuel, the system could effectively overcome the old system issues [4].

2.2   Hybrid Power Systems

Throughout the last two decades, the global awareness towards environmental issues has grown rapidly. Using fossil fuels as the main energy resource in power generation did not only caused a destructive environmental effects but also an increasing consumption of the world non-conventional energy sources. Proposing conventional

power sources such as solar energy (photovoltaic power generation) and wind energy (micro wind turbine power generation) as a solution for the power demand initiated a global movement towards the renewable energy [5].

Moreover, stand-alone hybrid power system represents the most common system used nowadays for supplying small villages, offshore installations, and off-grid industrial areas with electricity. The hybrid power system usually mixes two or three different power source to ensure reliability and continuous supply to the loads. For instance, the hybrid power system can have a conventional and non-conventional power sources that can work simultaneously or rotationally to supply the loads with the required demand without any disturbances or power shortages. Many researches, field experiments, and applications have been conducted towards the hybrid system approach as a result of the higher reliability and capability the system shown comparing with conventional systems [5].

A better understanding of the hybrid system characteristics will lead to an accurate implementation, evaluation and optimization of the system. Several researches have been introduced to discuss about hybrid systems. The main focus of these researches are about the potential of the hybrid system energy sources, the integration between two or more different sources and the performance analysis of the system.

This chapter presents a literature review on the hybrid system from different approaches: solar energy potential analysis, wind energy potential analysis, battery performance and storage system and the optimum sizing and designing methods for building a hybrid solar-wind-diesel system which combines three different energy sources.

2.2.1 Solar Photovoltaic Cell

Operating Principle of a Photovoltaic Cell

The power of the sun has been utilized into daily applications throughout the history. From heating, fire, and lighting, the power of the sun shaped the human history and contributed in the advancement and comfortability of human beings. The availability to generate electricity from the sun which also known as the photoelectric effect has been discovered in the eighteenth century. Solar cells have been utilized to convert the radiation of solar energy to direct current (DC) of electrical power [6].

6

Modern solar panels are mainly made of semiconductor materials such as silicon which considered the most dominant element in producing solar panels. The connection of solar panel arrays can be in series to generate higher voltage or in parallel to result in higher current. A solar PV module consists of series connected solar panels which can further be connected to parallel modules of panels to form a PV array of parallel and series solar panels [6].
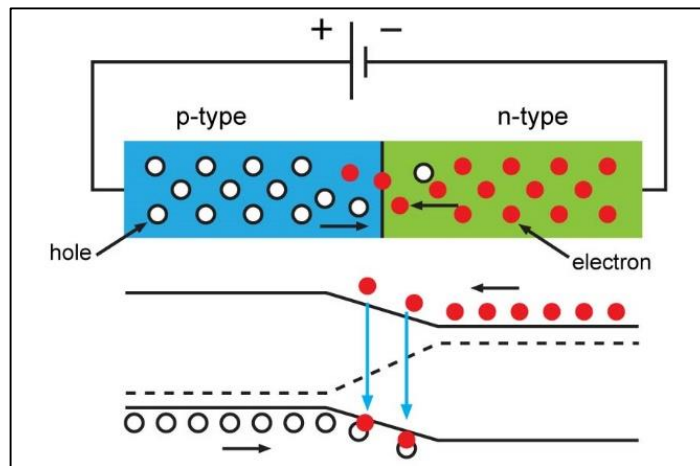
Figure 1 P-N junction operation in a solar cell [6]

The principle of operation for a solar panel is illustrated in Figure 1. The photoelectric effect depends on the P-N junction and the diffusion current resulted from the effect of solar radiation on P-N junction in semiconductors. Basically, in no-light mode, solar panels operate in the reverse direction and hence a drift current will be initiated between the P-N junctions. When solar panels are exposed to light, cell photons with energy greater than the P-N junction gap energy are absorbed and hence electron hole pairs are formed. These carriers are separated under the influence of electric fields within the junction, creating a current that is proportional to the incidence of solar irradiation [7].

Solar Cell Characteristics

Solar cells usually shows a nonlinear characteristics between generated power and cell voltage P-V curve and also between generated current and cell voltage I-V curve. The general I-V curve is shown in Figure 2. Basically, a solar cell has fundamental parameters which form the solar cell characteristics and behavior upon exposing to light or radiation. Theses parameters are short circuit current (I_{sc}), open circuit voltage (V_{oc}), maximum power point tracking algorithm (MPPT), and efficiency of the solar cell (η) [8].
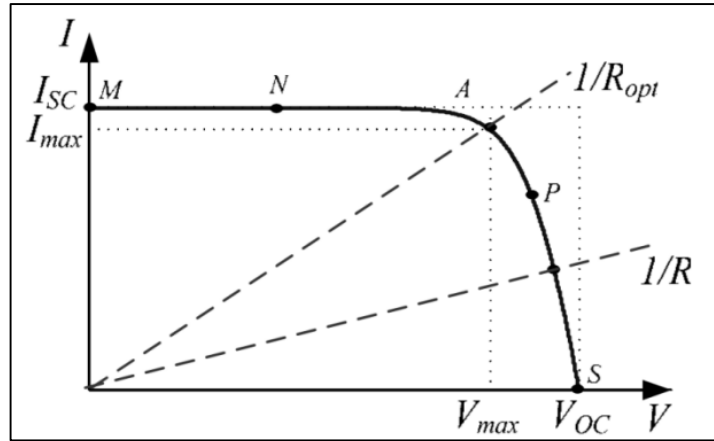
Figure 2 General I-V characteristics graph for a solar cell [9]

1. $I_{sc} = I_{ph}$: Short circuit current value is the highest value of current produced by a solar photovoltaic cell when the cell is in open circuit condition (V=0)

2. V_{oc} : Open circuit voltage is the highest voltage drop across the P-N junction of the solar cell (I_cell = 0). Mostly the Voc voltage will be presented during night time when there is no radiation level to create the photoelectric current.

3. MPPT: Maximum power point tracking is the operating point in the I-V curve where the maximum output power is generated from the photovoltaic cell. Also, it represents the point which have maximum voltage and maximum current as well.

2.2.2 Wind Turbines

Wind turbines were utilized by humans since the beginning of the modern industrial era. In the eighteenth century, wind turbines have been used mainly in agriculture environment for simple applications such as grinding or water pumping. In the nineteenth century, wind turbines were used to generate electricity for small houses and industrial areas by utilizing the wind speed to rotate the generator shafts. However, the discovery of fossil fuels and the new industrialization era resulted in significant decline in using wind turbine for energy generation. The fluctuating low output power provided by the classical wind turbines were substituted with the high efficient fossil fuels turbines that supplied a much higher output of consistent power [10].

In 1972, and followed by the first oil price shock in the twentieth century, renewable energy industry was emerged to find solutions sustainable power sources other than fossil fuels. Fossil fuels are burnt to generate mechanical energy that rotates the generator blades and hence supplying electricity. The disastrous environmental effects of using fossil fuels as the main power supply for electricity are devastating. Also, the global warming has achieved hazardous levels that can damage the environment due

to the excessive usage of fossil fuels. Wind turbines industry was initialized as a major potential source in providing renewable energy. Recently, the research and development in utilizing the wind power has witnessed a significant increase due to the environmental as well as the economic advantages over fossil fuels [11].

The wind power is clean, consistent, achievable, and the continuous development in creating efficient wind turbines has led to cheap and affordable systems [12]. The statics claim that there is a 90 % decrease in the cost of wind power generation since 1980 [13]. Wind turbines are considered one of the main renewable energy source nowadays and has been accepted to be an achievable alternative for fossil fuels [14].

Definition of a Wind Turbine

A wind turbine is a machine that converts the kinetics energy of the air into mechanical energy by utilizing the rotation of the wind turbine blades to generate a mechanical torque on the turbine shaft. If the turbine torque is used directly in pumping water or in agriculture purposed, the machine is called wind mill. However, if the turbine used as a prime mover for an electric generator to generate electricity, the machine is called wind turbine [15].
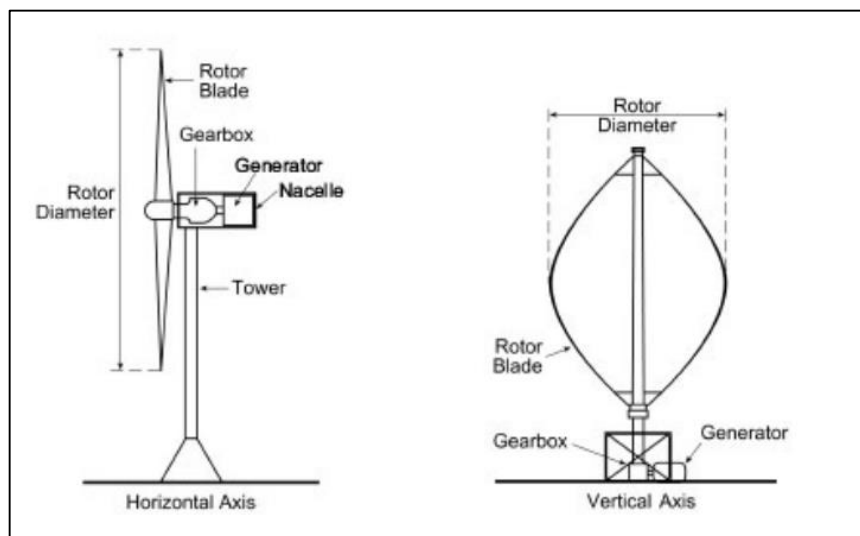
Figure 3 Vertical axis and horizontal axis wind turbines [15]

Horizontal-Axis and Vertical-Axis Wind Turbines

Wind turbines are classified into vertical axis wind turbines and horizontal axis wind turbines. Vertical axis wind turbines do not require any towers and the generator, gear boxes, and turbine control system can be installed on the ground. But, a vertical axis wind turbine will require an excitation system as it is not a self-starting machine. Moreover, controlling the amplitude and the frequency of a vertical axis wind turbine

9

will be difficult and hence the power efficiency will be affected significantly. Currently, horizontal axis wind turbines are the most affordable type of wind turbines available in the market. Figure 3 illustrates the different configuration between a horizontal-axis and a vertical axis turbine. A horizontal axis wind turbine mainly consists of [16]:

- Rotor blades that extract the kinetic energy in the wind and transform it to mechanical torque.
- The nacelle which is attached to the rotor blades and consists of the wind turbine rotor shaft, gear box system to regulate the wind speed, mechanical drivetrain system to drive the wind speed and accelerate the shaft to generate electricity, and finally an electric generator to transform the mechanical torque into electrical power supply.
- The turbine tower that support both the rotor blades and the nacelle.

The internal structure of a horizontal axis wind turbine is shown in Figure 4.
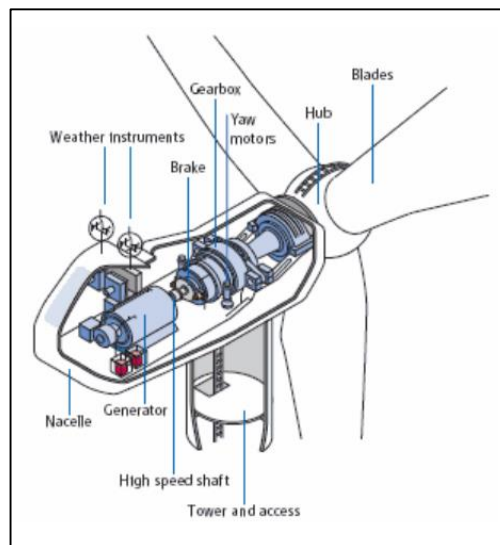
Figure 4 Internal structure of a horizontal axis wind turbines [16]

Rotor blades differ in shape, size and number per turbine. A wind turbine can have three blades, two blades, or sometime a single rotor blade. Usually, for generating electricity, a typical wind turbine will be equipped with two or three rotor blades. Also, a wind turbine with a two rotor blades will cost less than another turbine with three rotor blades. However, a two blades wind turbine will require a higher rotational speed to achieve the same output power for a three rotor blades turbine. On the current days, three rotor blades wind turbines are the most common type in wind turbine industry.

Variable-Speed and Constant-Speed Wind Turbines

Prior to the rising in the wind energy industry in the 1970s, Wind turbines were operated by fixed speeds. The rotor blades of the turbine were adjusted to a nominal value of wind speed and hence the generator was driven by the mechanical torque resulted from this speed. However, there were several disadvantages for fixes speed wind turbines such as lower efficiency, lower generated power, and wasting the potential of using high wind speed to generate more power form the turbine. In the other hand, there was a significant development in the field of power electronics, power converters, and rectifiers. This advancement paved the way for variable speed wind turbines to take over the wind energy industry later in the 1990s and after [15].

Variable speed wind turbine are the most dominant type of wind turbines nowadays. A power electronics convertor is mainly used to regulate the turbine output voltage according to the input wind speed to the turbine blades. In addition to that, the power convertor will help in controlling the fluctuating frequency of the system which will enable wind turbines to connect with the utility grid system. Despite the cost of power electronics system, a variable speed wind turbine can be operated in the maximum aerodynamic efficiency unlike the fixed speed wind turbines [17].

2.2.3 Diesel Generator

In the recent days, and with expansion of using renewable sources in generating green energy, diesel generators is believed to be one of the most essential components in a hybrid power system. According to Quebec government, the wind-diesel energy system has been officially adopted to be running through small and remote areas for supplying electrical energy and provide communication in northern areas of Quebec [18]. A diesel generating system is widely known to be one of the best energy generation systems. It has been used to supply electricity for remote areas, offshore constructions, and off-grid societies. The system has always showed robust and consistent performance [19]. However, due to the new policies of green energy production, diesel generators is believed to have a bright future as a main element in hybrid systems. A detailed study and efficient modelling of a diesel generation set can contribute to the analysis of the generator performance and reliability in order to design a more suitable generators for hybrid system applications [20].

The selected model of generation's sets for the project are diesel generators. The generator is a low speed 4-pole synchronous generator with diesel as a main fuel

system for the prime mover engine. Diesel generator are selected based on the availability, efficiency, robust design of the machines, and the ability of the generators to work in hazardous areas with harsh environments such as the offshore environment. Also, diesel fuel are prefers due to the fact that it can be stored for extended period of time. The generation set proposed in the project consists of a diesel engine with a low speed synchronous generator rotating in the same shaft. The engine is used to produce mechanical energy which is transferred to the rotor of the synchronous machine via the rotating shaft between the two sets. Finally, the generator converts the mechanical energy to electrical energy [21].
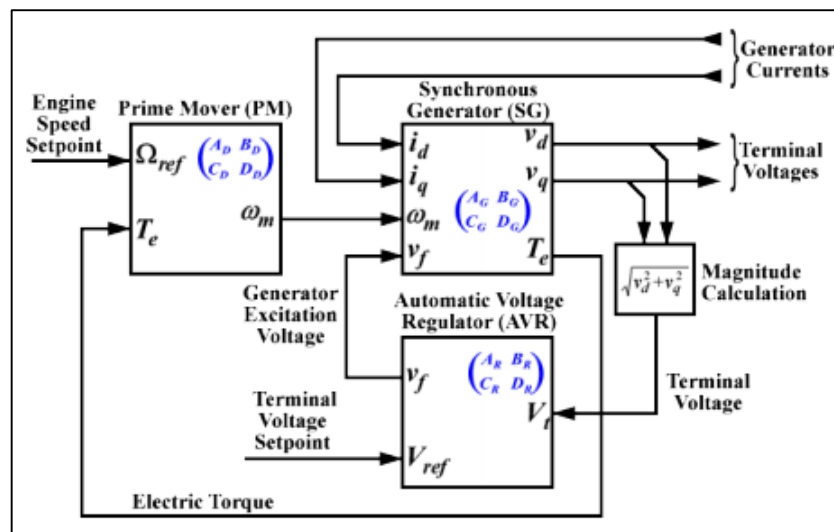
Figure 5 Diesel generator topology and interconnections

A synchronous generator has been implemented in the project due to the low cost for maintenance and operation, smooth operation, and availability. Moreover, alternators have been used extensively in hybrid systems for wind generations, hydropower generation, and emergency considerations [22]. Also, synchronous generators represent a higher efficiency in standalone systems due to the stabilized frequency and voltage the generators can achieve comparing to induction generators which require a much more complicated control system for stabilizing the frequency and voltage. In addition to that, synchronous generators can be used efficiently with prime movers that utilized biogas, diesel, natural gas or any source of mechanical rotation [23]. The diesel generator topology and interconnections is shown in Figure 5.

2.2.4 Energy Storage System (Battery System)

The modelling and simulation of an autonomous off-grid hybrid power system requires an energy storage and dumping system in order to usefully manage the generation units, AC and DC loads, and the excessive or shortage of power in the system during different operation durations and conditions. A battery system needs to be implemented in the hybrid power system along with the renewable energy units as well as the emergency diesel generator. Hence, various battery models have been investigated and examined to be used in the project such as the Peukert model, Doyle electrochemical battery model, the KiBaM model, and finally the generic battery model developed by Matlab/Simulink software application [24]. The previous models are distinguished by the lifetime of the battery, the accuracy, the battery material, and the accuracy of the charging process. Consequently, in this project, the generic battery model developed by Matlab/Simulink is being implemented. The generic battery model is designed and modelled to allow different battery models with characteristics that can be easily obtained from the manufacturer's datasheets. Moreover, the model validity has been verified [25].

2.3   Solar and wind energy potentials in Malaysia

Meteorological data such as solar radiation, wind speed, and temperature profiles differs from location to another. In order to effectively analyze the potential of solar and wind energy for the project location, the meteorological data for the location should be investigated to determine the energy profile of this area.

2.3.1 Solar Energy Potential Analysis in Malaysia

In recent years, the Malaysia government, universities, and researchers have paid increasing attention to solar and wind energy applications in Malaysia. Solar energy is a non-conventional power source that uses the solar irradiation to generate electricity. The phenomena is usually known as the photoelectric effect and it generates electrical currents based on the irradiance effect of the sun. During the last 50 years, the ability to use solar power has greatly increased and developed. This gave a promising future towards implementing the solar power in residential areas, factories, and off-grid communities. Also, the development in the semiconductor industry will change the old perception about the economic effect of using renewable energy over the conventional power sources [26].

In Malaysia, the research, development, and implementation of renewable energy sources has started only in the last 25 years. According to the world solar radiation distribution, the solar radiation levels in Malaysia are considered amongst the lowest radiation levels in the world. Figure 6 and Figure 7 showed that Malaysia has a mean solar radiation of 4.0 – 4.9 kWh/m2/day while the mean solar radiation level for the most countries in the world is around 6.0 – 6.9 kWh/m2/day [27].
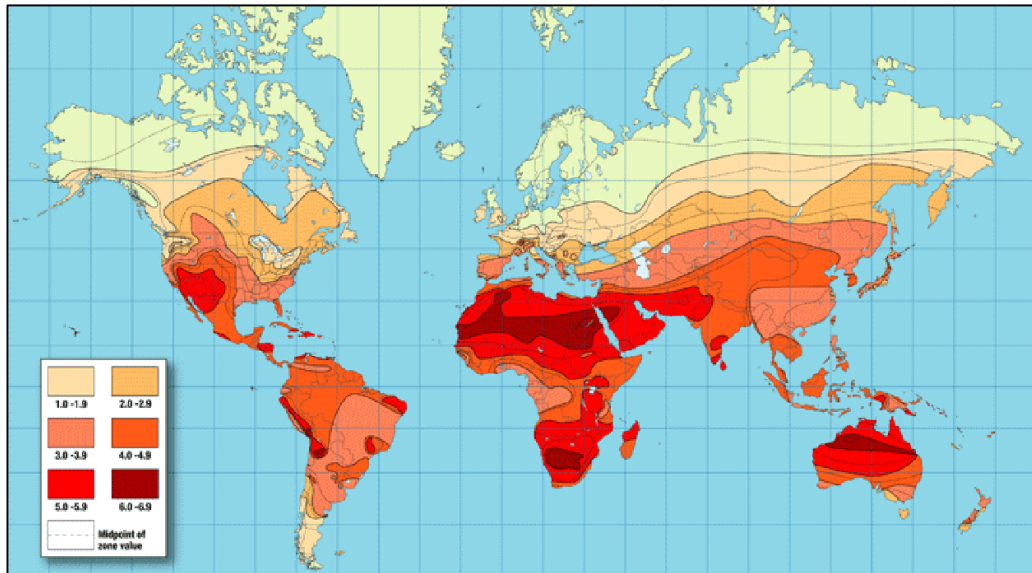
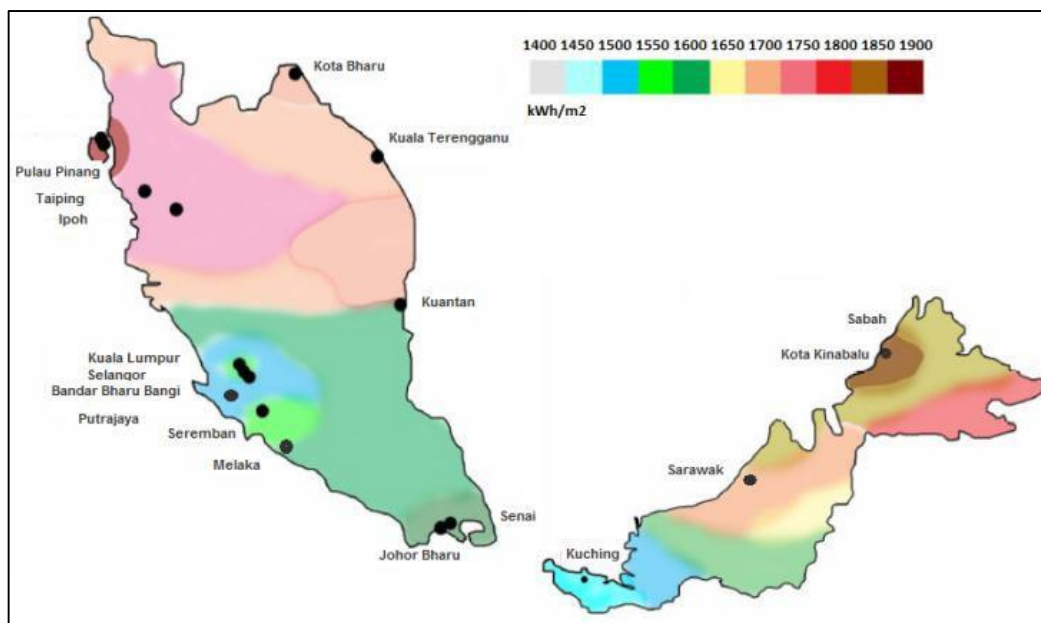Figure 6 World daily solar radiation map [27]

Figure 7 Annual average daily global solar irradiation in Malaysia [28]

In the recent era, solar energy is considered as the main and the most dominant source of renewable energy. The reason behind this consideration is that solar energy is predictable and constant for all the locations in the world. There are two main

technologies which are used to capture the solar effect and generate electricity. The first one is the photovoltaic solar panels which convert the irradiance of the sun into a DC electrical current. The continuous development in the field of power electronics has resulted in significant generation capability of the PV panels which can convert 5-15 % of the sun irradiance into DC currents [29].

The second method used for generating electricity is solar thermal effect which uses the sun to heat water. The DC current generated by the photovoltaic solar panels can be stored into a storage system such as batteries or can be converted to AC current by using power converters. For a standard irradiance level of 800 W/m2 and during the standard operating conditions, a PV panel of 1 m2 can generate maximum 100 watt of power [29].

The efficiency and reliability of solar energy are affected by the ambient environment. The generation can be disturbed by the ambient temperature, the solar radiation levels, the climatic conditions, and the arrangement of the photovoltaic system. The efficiency reduction due to high air temperature in Malaysia is estimated to be 8 % while the efficiency reduction due to the dust and other environmental disturbances is estimated to be about 2 % of the total rated generation capacity of the photovoltaic system. The standard life span of a photovoltaic panel is 25 years. On the other hand, The life time for the electronic power converters, batteries, and charge controllers is estimated to be from 5 to 10 years [29].

2.3.2 Wind Energy Potential Analysis in Malaysia

Wind energy term is used to describe the process of obtaining electricity from the wind movement. The conversion and generation of electricity occurs by using wind turbines or micro-wind turbines for smaller power capacity. Wind turbines is used to convert the kinetic energy of the wind flowing through the wind turbine blade into mechanical power used to rotate the wind turbines blades and consequently generates electricity [26].

The wind energy has grown to be a promising and reliable power source. The wind power is clean, achievable and maintainable. According to previous studies, the amount of wind power installation around the globe is estimated to be 58.982 MW. This is almost 2 % of the total production capacity worldwide [30].

In the offshore environment, wind power is considered to be much more powerful than onshore environment. Wind farms are installed for generating electricity to off-grid offshore installations. A wind turbines farm will benefit from the wind speed available in the offshore environment and this will help to generate more electricity comparing to onshore wind farms [31].

Researches have been conducted to maximize the wind energy output in Malaysia. The studies show that only few places are sufficient for the establishment of wind farms. The current wind farms installation are mainly located in Sabah and Sarawak. In order to ensure the reliability and high performance of a wind turbine, there are many design aspects needs to be taken into consideration such as the ambient environment and the wind speed analysis [31].

The analysis of a potential site for a wind turbine is essential in investigating about the feasibility of project. Wind speed, wind flow dynamics, and climatic conditions are among the most crucial factors designers rely on during the pre-feasibility study of the project. The meteorological data needed for the study can be obtained and sourced from the national meteorological center in Malaysia [32, 33].

Figure 8 indicates the most promising locations for wind energy in Malaysia. The selected locations were numbered where location 1-7 represent the possible location on eastern peninsular Malaysia seashore. The numbers from 8-10 represents the possible locations onshore and offshore the coastline of Sabah and Sarawak state [34].

According to the studies, sites 1, 2, 3 and 8 were found to be more feasible for the project. The main criteria for the selection is that during the annual northeast monsoon season, the wind speed in these areas will excess 5 m/s. although this is a significant achievement in wind speed needed for the project, but the sites experienced lower wind [34].
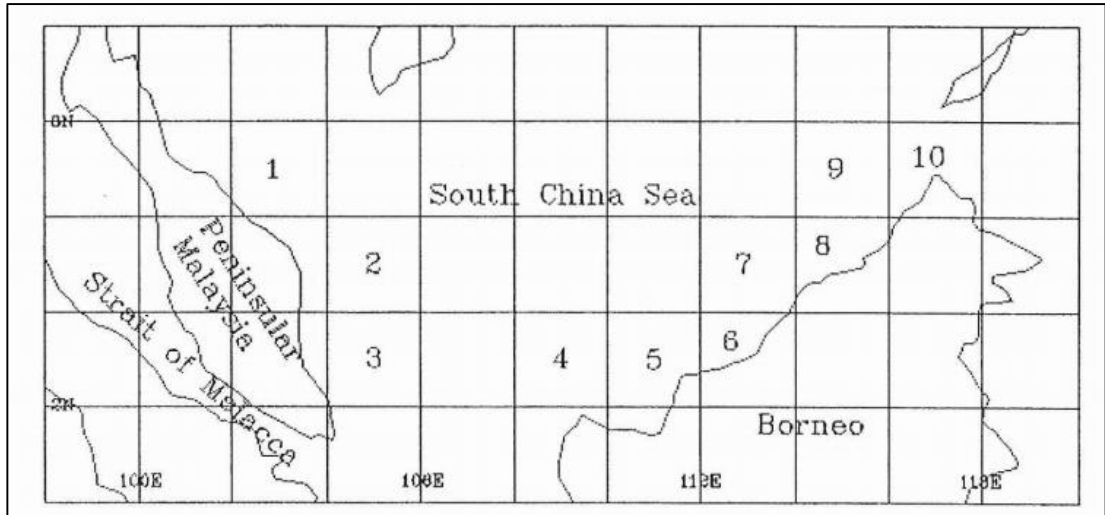
Figure 8 Selected locations for potential wind energy

CHAPTER 3 : RESEARCH METHODOLOGY

In this chapter the project research methodology is explained in detail. The methodology was developed based on the literature review and the pre-feasibility study of the project. Figure 9 illustrates the general steps of the project methodology.

Hybrid Power System Feasibility Study

Investigation on Unmaned Installations Power Demand

Modelling and Simulation of Solar Photovoltaic Panels

Modeling and Simulation of a Micro-Wind Turbine

Modelling and Simulation of a Diesel Generator Set

Developing Energy Storage and Control Strategies

Developing a Complete Hybrid Power System Model

Optimization Study for the Hybrid Power System

Figure 9 Research methodology

3.1 Unmanned Installation Power Demand

In designing an unmanned offshore platform, the load profile represents one of the most crucial elements in the design process. Sizing the power system must ensure that the load profile is covered under all the situations and circumstances. Moreover, by implementing a renewable power system to fully supply the platform loads, the load data needs to be analysed. Based on the existing North Sea unmanned platform Cutter, the DC load data will vary between 250 W to 400 W and the probability of higher load is considered rare and unlikely to occur. The average daily demand of current on-board

the platform for the instrumentation devices is 13.85 A for a DC voltage value of 24 V as specified by SHELL, the owner company of the platform [35]. Consequently, the total average load for the platform are calculated from the following equations.

$$P_{watt} = I_{avg} * V_{avg} \qquad (3.1)$$

$$E_{kwh} = \frac{P_{watt}*t_h}{1000} \qquad (3.2)$$

Where: The energy (E) in kilowatt-hours (kWh) is equal to the power (P) in watts, times the time period (t) in hours (hr.) divided by 1000. Based on the equations, the total average load will be 332.4 W and this will result in a total energy consumption of 7.978 kWh/day.

3.2 Solar Photovoltaic Module

A simplest equivalent circuit of a solar cell is a current source in parallel with a diode. The output of the current source is directly proportional to the solar energy (photons) that hits on the solar cell photocurrent (*Iph*). During darkness, the solar cell is not an active device; it works as a diode, i.e. a p-n junction. It produces neither a current nor a voltage. However, if it is allowed to connect to an external source (large voltage) it generates a current (*Id*), called diode (*D*) current or dark current. The diode determines the *IV* characteristics of the cell.
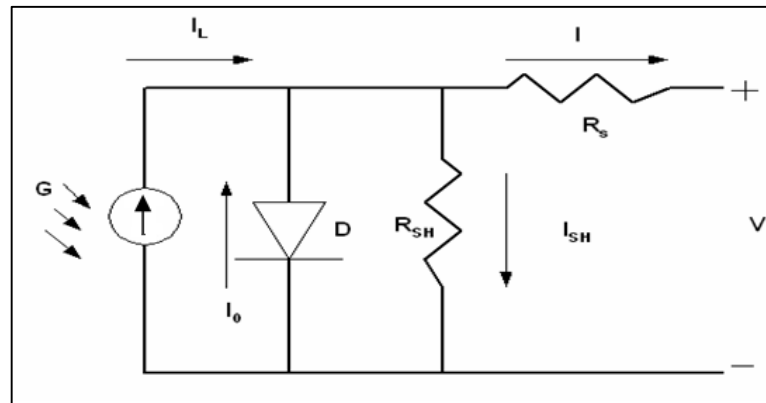
Figure 10 Solar cell electrical model [9]

The circuit diagram of a PV cell is shown in Figure 10. Accurate simulation is obtained after considering the following parameters:

- Temperature dependence of the diode reserved saturation current (I*s*).
- Temperature dependence of the photo current (I*ph*).
- Series resistance (R*s*), (internal losses due to the current flow) which gives a more accurate shape between the maximum power point and the open circuit voltage.

- Shunt resistance (R*sh*), in parallel with the diode, this corresponds to the leakage current to the ground.

Equations which define the model of a PV cell are given below:

$$V_T = \frac{K * T_{OP}}{q} \tag{3.3}$$

$$V_{OC} = V_T \ln \frac{I_{Ph}}{I_S} \tag{3.4}$$

$$I_d = [e^{\ln(\frac{V + I * R_S}{n * V_t * C * N_S})} - 1] * I_S * N_P \tag{3.5}$$

$$I_S = I_{rs} * \left(\frac{T_{op}}{T_{ref}}\right)^3 * e^{[\frac{q * E_g}{n * k}\left(\frac{1}{T_{op}} - \frac{1}{T_{ref}}\right)]} \tag{3.6}$$

$$I_{rs} = \frac{I_{sc}}{[e^{\left[\frac{q * V_{OC}}{n * k * C * T_{op}}\right]} - 1]} \tag{3.7}$$

$$I_{sh} = \frac{V + I * R_S}{R_P} \tag{3.8}$$

$$I_{ph} = G_k[I_{sc} + K_1(T_{OP} - T_{ref}] \tag{3.9}$$

$$I = I_{ph} * N_P - I_d - I_{sh} \tag{3.10}$$

Where:
- STC: Standard Test Condition, G=1kw/m2, $T_{OP} = 25°C$
- G_k : Solar irradiance ratio
- V_T : Thermal Voltage, V
- K : Boltzmann's constant, 1.38e-23
- T_{OP} : Cell operating temperature in °C
- T_{ref}: Cell temperature at 25°C
- q : Electron Charge constant, 1.6e-19 C
- I_S : Diode reversed saturation current, A
- I_{rs} : Diode reversed saturation current at T_{OP}
- I: Output current from the PV panel, A
- I_{sh}: Shunt current, A
- V: Output voltage from the PV panel, V
- n: Diode ideality factor,1.36
- C: No of cells in a PV panel, 36

- N_S, N_P: No of PV panel in series & parallel
- E_g: Band-gap energy of the cell, 1.12eV

3.2.1 DC-DC Buck Convertor

In order to control the solar panels array output voltage, a DC-DC buck convertor is used to step down the output voltage, hence enable a more efficient and accurate method of controlling the output power of the array. The DC-DC buck convertor consists of input voltage source (Vs), switching device to control the output voltage (S), diode (D), high value inductor (L), filter capacitor (C) and output load resistance (RL). The basic structure of the DC-DC buck convertor is shown in Figure 11.
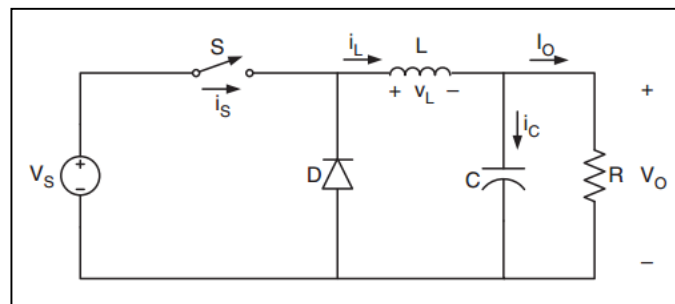
Figure 11 DC-DC buck convertor

The buck convertor is assumed to be working in continuous conduction mode CCM. Consequently, the inductor current (I_l) is always positive during the on state of the buck convertor. In the on state of the controlled switch S, the diode D is reverse biased. When the controlled switch S is on the off state, the diode D will be forwarded biased and the will supply the load resistance with uninterrupted current through the inductor.

The input-output voltage relationship can be defined by using inductor voltage (V_d) which, according to Faraday's law, has a value of zero over steady state analysis (constant time).the following equations are used to define the duty cycle ratio used in the operation of the buck convertor:

$$(Vs - Vo)DT = -Vo(1 - D)T \tag{3.11}$$

Hence,

$$\frac{Vo}{Vs} = D \tag{3.12}$$

Where:

- Vo: Output Voltage
- Vs: Input Voltage
- D: Ratio of output voltage to input voltage

- T: Duty cycle

The following equations will be used to determine the parameter of the buck convertor:

$$L_{crit} = \frac{1-D}{2} * TR \hspace{4cm} (3.13)$$

$$L = 100 * L_{crit} \hspace{4cm} (3.14)$$

$$C_{min} = \frac{(1-D)*V_o}{8*L*f^2*V_s} \hspace{4cm} (3.15)$$

Where:

- Cmin: The minimum value used for filter capacitance (uF).
- Lcrit: The minimum value to ensure that the buck convertor is working on CCM (H).
- L: the typical value sued for the inductance in the buck convertor circuit (H).
- T: switching period (sec).
- R: Output load resistance (ohm).
- F: Switching frequency (kHz).

Simulink average based model is used to replace the controlled switch S in the design. Moreover, a smoothing capacitor (Cin) will be used to filter the input voltage. To ensure the highest output power from the solar panels array, the switching frequency needs to be adjusted according to the irradiation level as well as the load resistance. In case of using fixed frequency, fixed duty cycle, to switch the convertor, the output power will be varied according to the load value and the irradiation level. Hence, a MPPT algorithm will be presented to overcome this issue and sustain the maximum output value of the solar panels array system.

3.2.2 Maximum Power Point Tracking (MPPT) Algorithm

MPPT are various techniques and algorithms used to sustain the highest obtainable value of the output power from a solar photovoltaic cell, panels or array. There are various techniques used to regulate the output voltage and current to preserve the maximum output power under varied loads or irradiation levels.

In this paper, a MPPT algorithm utilizing fractional open circuit voltage technique will be used. Basically, the technique define the relationship between the solar photovoltaic cell open circuit voltage Voc and maximum obtainable voltage Vmpp under standards operating conditions. For every irradiation level and operation temperature, there are a specific value of Vmpp that can be achieved to produce the maximum output power

Pmpp. This value represented a fractional value of the open circuit voltage of the solar photovoltaic cell. Consequently;

$$\frac{Vmpp}{Voc} = K, \ 0 < K < 1 \tag{3.17}$$

Where; K is the fixed fractional value to be used for sustaining the maximum output value of power generated by the solar photovoltaic system Pmpp. The fractional value K is estimated to be 0.82 for Solarex-MSX60 60Wp Solar Module used in this paper. The following flow chart represents the basic operating principle of the open circuit voltage MPPT algorithm. The project MPPT algorithm is shown in Figure 12.
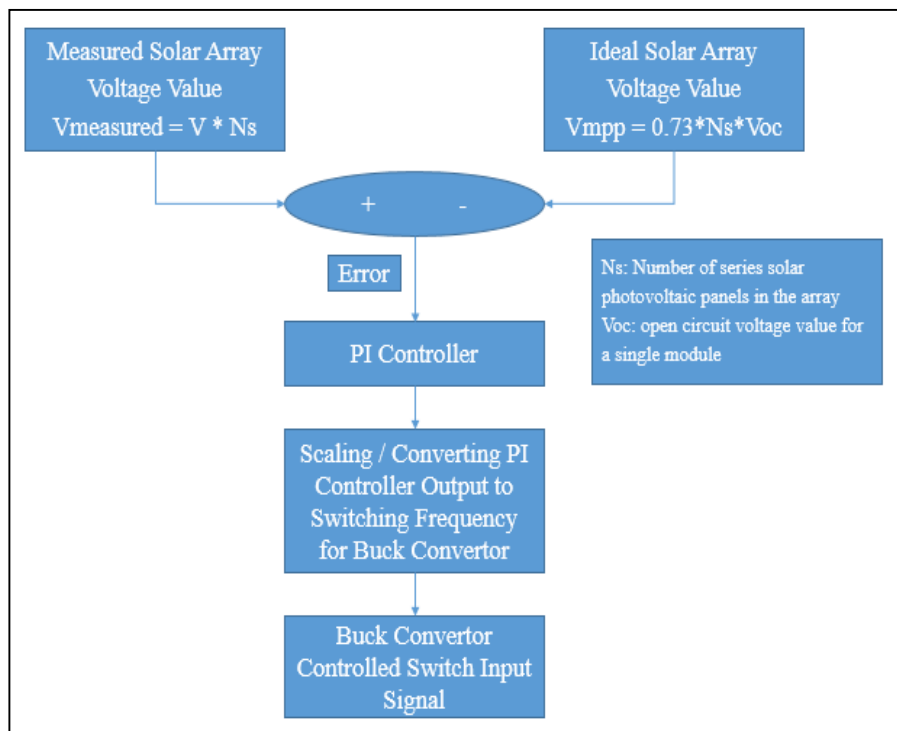
Figure 12 Fractional open-circuit voltage MPPT algorithm flowchart

Despite being efficient and uncomplicated in implementation, the fractional value K is difficult to adjust and hence a PI controller will be added to the design to dynamically achieve the maximum output voltage Vmpp.

3.2.3 Proportional Integral (PI) Controller

The fractional open circuit voltage algorithm will be used as a reference input to the PI controller implemented in the design. The PI controller will tune the error resulted from the difference between the ideal Vmpp value for the Solar array used and the measured value from the system. Then, the controller output will be scaled and used as a switching frequency for controlled switch used in the buck convertor circuit.

The proportional integral controller (PI) controller is used to tune and eliminate the error exist by varying the load as well as the irradiation levels on the solar photovoltaic array system. Moreover, the solar photovoltaic system will trigger the controlled switch S in the buck convertor to dynamically compensate the switching frequency and preserve the maximum output power Pmpp at the load resistance. The state space representation of the buck convertor was used to obtain the transfer functions of the buck convertor, hence calculating the integral gain (Ki) and the proportional gain (Kp) needed for the PI controller tuning algorithm. The transfer functions used in the paper are illustrated below with reference to the S-domain.

$$I_l(S) = \frac{1}{L*S}[D * V_S(S) - V_o(S)] \tag{3.18}$$

$$V_S(S) = \frac{1}{C_1*S}[I_{PV}(S) - D * I_l(S)] \tag{3.19}$$

$$V_o(S) = \frac{1}{C_2*S}[I_l(S) - \frac{V_o(S)}{R_l}] \tag{3.20}$$

Where:

- L: inductor value
- C_1 : Input capacitor
- C_2: Output capacitor
- R_L: output load resistance

The transfer function H(S) used for the PI compensation is obtained by dividing the output voltage (Vo) to the input voltage (Vs) as illustrated below.

$$H(s) = \frac{V_o(s)}{V_S(s)} = \frac{RD(K_p*S+K_i)}{R*L*C_2*S^3+L*S^2+R*S+RD(K_p*S+K_i)} \tag{3.21}$$

Where, Ki : Integral gain, Kp: Proportional gain.

3.2.4 Solar Photovoltaic Simulation Modules

The simulation of the model was carried out in three main stages in accordance with the advancement of the model design. Matlab/Simulink environment was used to simulate the behavior and characteristics of the solar modules in the paper. PI controller Simulink block was used to tune the error and maintain the maximum output power Pmpp in the output terminals of the buck convertor.

The first model was developed to prove the operating characteristics of the Solarex-MSX60 60Wp Solar Module. The model contained input data from the solar module datasheet and presented the behavior of the solar panel under standard test conditions and with no load attached to that solar module. The output results from the first module were used to study the effect of variable resistance to the operation of the solar cell in the second model. Table 1 includes all the parameter obtained from the first model simulation. The parameters are calculated based on the equations in section (3.2).

Table 1 Calculated parameters for the first PV model

Parameter	Calculated Value
Iph	3.965 (A)
Vt	0.0322 (v)
Is	$1.139 * 10^{-5}$ (A)
Irs	$5.812 * 10^{-6}$ (A)
Voc	21.1 (v)

The second model was built to simulate the effect of variable resistance on the solar module. A single solar module was used in the second model. Furthermore, the results obtained from the first model was inserted in the second model and the behavior of the variable load was obtained by using Simulink Scope block. A ramp function was used to vary the resistance according to the slope identified in the Simulink ramp function block.

Finally, the third and final model was developed using the input data from the first and second models. Unlike the first and the second models, which consisted only of one solar module, the third model represents a photovoltaic system of two parallel arrays with ten solar modules in each array connected in series. The photovoltaic system presented in the third model will be controlled by buck convertor to enable MPPT algorithm as illustrated previously. To ease the calculations in the third model, a similar mathematical model derived from the original model was developed to represent a single solar module. The equation used in the third model solar modules is:

$$I = Iph * Np - Is * Np \left(e^{\frac{V + I * Rs}{n * Vt * C * Ns}} - 1 \right) - \left(\frac{V + I * Rs}{Rp} \right) \tag{3.22}$$

Where:

- I: Solar module output current (Amps).
- Iph: Diode current (Amps).
- Np: Number of arrays in parallel.
- Ns: Number of series solar modules in the array.
- N: Fill factor
- C: Number of solar photovoltaic cells in each modules.
- Vt: Thermal voltage (Volt).
- Rs: Solar photovoltaic cell parallel resistance (Ohm)
- Rp: Solar photovoltaic cell series resistance (Ohm)
- V: Output Voltage (Volt)

3.3 Wind Turbine Module

Modern wind turbine generator systems are constructed mainly as horizontal axis of rotation, a wind wheel consisting of three blades, a high speed asynchronous generator (also known as induction generator) and a gear box. The wind turbine under study falls in this category and is also equipped with a blade pitch angle control system, which enables the power generated by the wind turbine to be controlled.

3.3.1 Wind Turbine Rotor Blades

The following equations are used to model the blades mechanism and to identify the mathematical relationship between the wind speed and the generated mechanical power.

$$E = 0.5 * m * v^2 \tag{3.23}$$

$$P_W = \frac{dE}{dt} = 0.5 * m * v^2 \tag{3.24}$$

$$P_W = 0.5 * \rho * A * v^3 \tag{3.25}$$

$$\rho = \rho_0 - 1.194 * 10^{-14} * H \tag{3.26}$$

$$\rho_0 = 1.225 \frac{kg}{m^3} \, at \, T = 298K \tag{3.27}$$

$$P_{Blade} = C_{P(\lambda,\beta)} * P_W = C_{P(\lambda,\beta)} * 0.5 * m * v^3 \tag{3.28}$$

$$\lambda = \frac{\omega_m * R}{v} \tag{3.29}$$

$$T_w = \frac{P_{Blade}}{\omega_m} = C_{P(\lambda,\beta)} * 0.5 * \rho * A * v^3 \tag{3.30}$$

Where:

- E: The Kinetic energy in air
- m: Mass flow rate (Kg/Sec)
- v: Wind speed (m/s^2)
- P_W: The Power in the moving air (Watt)
- ρ: The Air density (kg/m3)
- ρ_0: Air density at sea level at temperature T=298K, $\rho_0 = 1.225$ kg/m3.
- H: Height above Sea level (m)
- P_{Blade}: The power extracted from the wind (Watt)
- λ: The tip speed ratio (Unitless)
- ω_m: Angular velocity of the rotor (Rad/Sec)
- R: Rotor radius (blade length) in meter
- T_w: The Rotor torque to the generator (N.m)

3.3.2 Mechanical Drivetrain

The mechanical drivetrain will be accomplished using two-mass model which will transform the mechanical torque of the wind turbine into the electromechanical torque of the synchronous generator used in the model. The mechanical torque of the wind turbine and the electromechanical torque of the generator act against each other which will result in positive sign for the wind turbine torque and negative sign for the electromechanical torque of the synchronous generator. The mechanical drivetrain for the small-scaled wind turbine are modelled based on Figure 13.
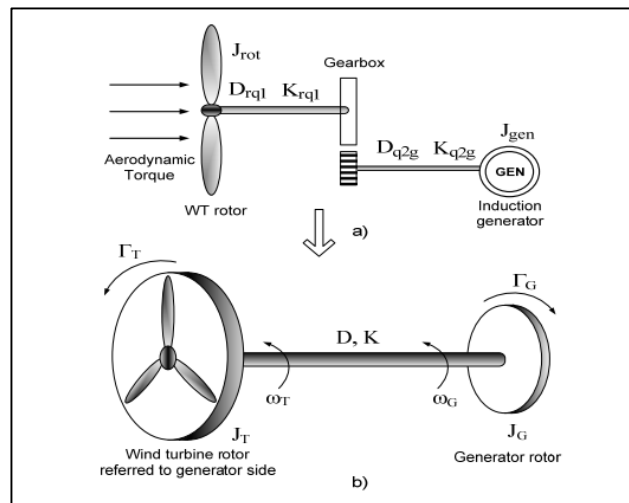

Figure 13 Wind turbine mechanical drivetrain model [36]

$$\tau_T = J_T \ddot{\theta}_T + D(\omega_T - \omega_G) + k(\theta_T - \theta_G) \tag{3.31}$$

27

$$-\tau_G = J_G\ddot{\theta}_G + D(\omega_G - \omega_T) + k(\theta_G - \theta_T) \qquad (3.32)$$

$$\frac{d}{dt}(\theta_G - \theta_T) = (\omega_G - \omega_T) \qquad (3.33)$$

$$\dot{\omega}_T = \frac{1}{J_T} * \left(\tau_T - D(\omega_T - \omega_G) - k(\theta_T - \theta_G)\right) \qquad (3.34)$$

$$\dot{\omega}_G = \frac{1}{J_G} * \left(-\tau_G + D(\omega_T - \omega_G) + k(\theta_T - \theta_G)\right) \qquad (3.35)$$

Where:

- τ_T, τ_G: wind turbine aerodynamic and generator electromagnetic torque [Nm]
- J_T, J_G: Moments of inertia of the wind turbine rotor and the generator [kgmm]
- D, k : equivalent damping and stiffness [Nms/rad], [Nm/rad]
- θ_T, θ_G: angular position of the rotor and the generator [rad]
- ω_T, ω_G: Wind turbine rotor and the generator speed [rad/s]

3.3.3 Permanent Magnet Synchronous Generator

The Simulink model for the permanent magnet synchronous generator is shown in figure 14. The model utilizes a negative torque as an input for the synchronous machine which generate three phase voltage at its terminals.
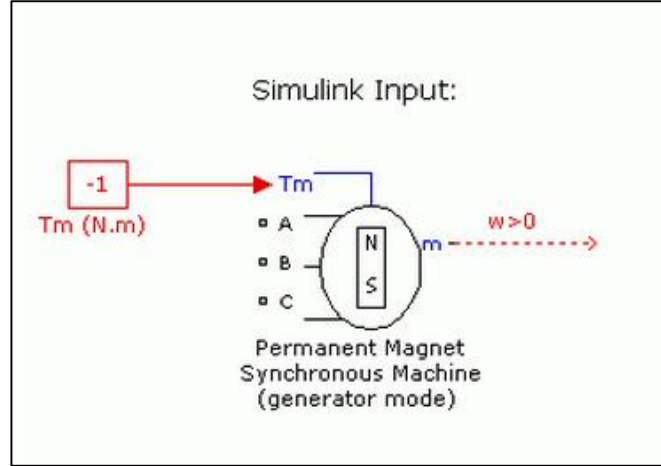

Figure 14 Permanent magnet synchronous generator model

Matlab/Simulink model for permeant magnet synchronous machine was implemented to transforms the mechanical torque generated by the wind turbine to three phase AC electrical power. The model parameters and equations are described below in the next part. Firstly, the three phase sinusoidal model of the generator electrical system is modelled using the rotor reference frame (d-q frame) and all the equations and parameters are referred to the rotor side:

$$\frac{d}{dt}i_d = \frac{1}{L_d} * v_d - \frac{R}{L_d}i_d + \frac{L_q}{L_d}i_q * p * w_m \tag{3.36}$$

$$\frac{d}{dt}i_q = \frac{1}{L_q} * v_q - \frac{R}{L_q}i_q + \frac{L_d}{L_q}i_d * p * w_m - \frac{\lambda * p * w_m}{L_q} \tag{3.37}$$

$$T_e = 1.5 * P[\lambda i_q + (L_d - L_q)i_q * i_d] \tag{3.38}$$

Where:

- L_q, L_d : q and d axis inductances
- R : Resistance of the stator windings
- i_q, i_d : q and d axis currents
- v_q, v_d : q and d axis voltages
- ω_m : Angular velocity of the rotor
- λ : Amplitude of the flux induced by the permanent magnets of the rotor in the stator phases

- p : Number of pole pairs
- T_e : Electromagnetic torque

The mechanical system for the same model are modelled as:

$$\frac{d}{dt}\omega_r = \frac{1}{J} * \left(T_e - T_f - F\omega_m - T_m\right) \tag{3.39}$$

$$\frac{d\theta}{dt} = \omega_m \tag{3.40}$$

Where:

- *J:* Combined inertia of rotor and load
- *F:* Combined viscous friction of rotor and load
- *Θ:* Rotor angular position
- *T_m:* Shaft mechanical torque
- *T_f:* Shaft static friction torque
- ω_m: Angular velocity of the rotor (mechanical speed)

3.4   Diesel Generator

Like various electromechanical power production systems, a diesel generator consists of three main parts, the first part is the diesel generator prime mover which includes the diesel engine with the generator speed governor. The second part is electrical generator which utilized the mechanical input power from the diesel engine shaft to transform the mechanical rotation energy to electrical energy. In this project, a salient pole synchronous generator was implemented to produce the electrical energy. The third part of the diesel generation system is the excitation system and the automatic voltage regulator, which both were implemented using AC5A IEEE system configuration and recommendations for per-unit systems.

The control strategy for the diesel generation set was achieved using diesel engine speed governor and synchronous generator automatic voltage regulator (AVR). The speed governor regulates the diesel engine rotation speed according to the pre-defined value and the actual rotation value measured at the generator terminals. In a similar approach, and to regulate the output voltage of the generator, automatic voltage regulator (AVR) is used to regulate and stabilize the output voltage of the synchronous generator via adjusting the excitation field voltage applied to the generator rotor via slip rings. In the next part, a detailed explanation of the modelling process of the diesel generator is illustrated.

3.4.1 Diesel Engine and Prime Mover

In diesel generator sets, diesel engine is the main purpose of providing impulsion. An engine governor is used to automatically adjust and control the diesel engine speed. The purpose is ensuring that the diesel engine can be at specific speed to stable operation. In this paper, the combination of diesel engine and governor used second-order transfer function for modeling. The following equations represents the controller transfer function and the actuator transfer function for a diesel engine and its governor system.

$$Hc = k * \frac{1+T3*s}{1+T1*s+T1*T2*s^2} \tag{3.41}$$

$$Ha = \frac{1+T4*s}{s(1+T5*s)(1+T6*s)} \tag{3.42}$$

Where:

- Hc: Controller transfer function.
- Ha: Actuator transfer function.

The model equations have been implemented using Matlab/Simulink environment. The model will measure the difference between the reference speed and the actual measure speed. Then, the error will be calculated and a PID controller is implemented to tune the error and dynamically adjust the mechanical output power supplied to the synchronous generator. Figure 15 shows the diesel engine governor model used in the project.
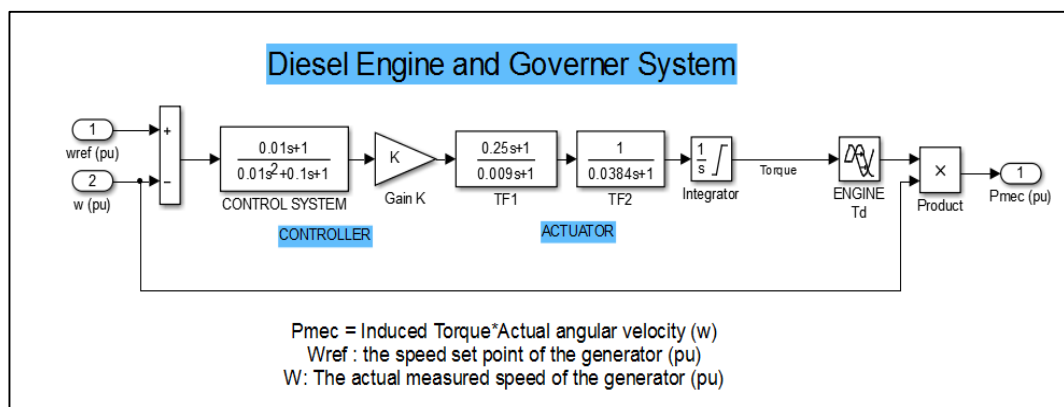

Figure 15 Prime mover Simulink model

Table 2 includes the control parameters used for the diesel generator prime mover.

Table 2 Prime mover controller and actuator parameters

Parameters	Value
Regulator gain K	15.62
Regulator time constants [T1 T2 T3] (s)	[0.1 0.1 0.01]
Actuator time constants [T4 T5 T6] (s)	[0.25 0.009 0.0384]

3.4.2 Synchronous Generator

The synchronous machine used in the model is a three-phase synchronous generator with its input port connected to the mechanical output power Pmec of the Prime Mover. Matlab/Simulink model was used to implement the synchronous machine taking into considerations per-unit values (pu) as measured values of the generator.

The synchronous machine block operates in generator or motor modes. The operating mode is dictated by the sign of the mechanical power (positive for generator mode, negative for motor mode). The electrical part of the machine is represented by a sixth-order state-space model and the mechanical part is the same as in the Simplified Synchronous Machine block.

The model takes into account the dynamics of the stator, field, and damper windings. The equivalent circuit of the model is represented in the rotor reference frame. All rotor parameters and electrical quantities are viewed from the stator. They are identified by primed variables. The subscripts used are defined as follows:

- D, q: axis quantities for dq representation.
- R, s: rotor and stator quantities for the synchronous machine.
- I,m: Leakage and magnetization inductance.
- F, k: field and damper winding quantities.

Figure 16 and 17 show the electrical model of the synchronous generator used in the model as well as the equations of the electrical model.
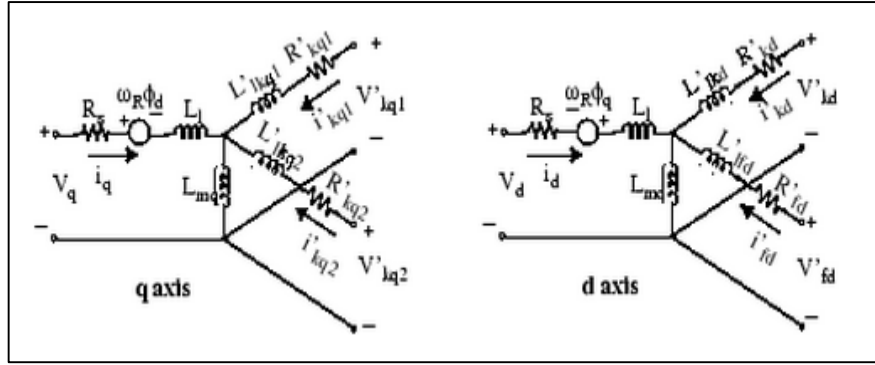
Figure 16 Synchronous generator electrical model

$$V_d = R_s i_d + \frac{d}{dt}\varphi_d - \omega_R \varphi_q \qquad \varphi_d = L_d i_d + L_{md}\left(i'_{fd} + i'_{kd}\right)$$

$$V_q = R_s i_q + \frac{d}{dt}\varphi_q + \omega_R \varphi_d \qquad \varphi_q = L_q i_q + L_{mq} i'_{kq}$$

$$V'_{fd} = R'_{fd} i'_{fd} + \frac{d}{dt}\varphi'_{fd} \qquad \varphi'_{fd} = L'_{fd} i'_{fd} + L_{md}\left(i_d + i'_{kd}\right)$$

$$V'_{kd} = R'_{kd} i'_{kd} + \frac{d}{dt}\varphi'_{kd} \qquad \varphi'_{kd} = L'_{kd} i'_{kd} + L_{md}\left(i_d + i'_{fd}\right)$$

$$V'_{kq1} = R'_{kq1} i'_{kq1} + \frac{d}{dt}\varphi'_{kq1} \qquad \varphi'_{kq1} = L'_{kq1} i'_{kq1} + L_{mq} i_q$$

$$V'_{kq2} = R'_{kq2} i'_{kq2} + \frac{d}{dt}\varphi'_{kq2} \qquad \varphi'_{kq2} = L'_{kq2} i'_{kq2} + L_{mq} i_q$$

Figure 17 Synchronous generator d-q equations

The synchronous machine block used in the diesel generator model is utilizing the Pu fundamental standard for the stator and rotor parameters. In Table 3 and 4 the formulas for the per-unit values are illustrated.

Table 3 Stator parameters in (Pu) representation

$R_{Z-Pu} = \dfrac{R_Z}{Z_{Sbase}}$	Stator resistance / phase
$L_{I-Pu} = \dfrac{L_I}{L_{Sbase}}$	Stator leakage inductance
$L_{md-Pu} = \dfrac{L_{md}}{L_{Sbase}}$	Direct axis magnetization inductance
$L_{mq-Pu} = \dfrac{L_{mq}}{L_{Sbase}}$	quadrature axis magnetization inductance

Table 4 Rotor parameters in (Pu) representation

$$R_{f-Pu} = \frac{R_f}{Z_{Sbase}}$$	Field resistance
$$L_{Ifd-Pu} = \frac{L_{Ifd}}{L_{Sbase}}$$	Field leakage inductance

The synchronous generator used in the diesel generation set is a 2000 VA generator with a nominal voltage of 480 V and frequency of 60 Hz. The generator parameters used in the model are shown in Table 5.

Table 5 Synchronous generator parameters

Parameter	Value
Rotor Type	Salient-Pole
Nominal power, line-to-line voltage, frequency [Pn(VA) Vn(Vrms) fn(Hz)]	[2000 480 60]
Reactances [Xd Xd' Xd" Xq Xq" Xl] (pu)	[0.078, 0.296, 0.252, 0.003, 0.243, 0.18]
Time constants [Tdo' Tdo" Tq"] (s)	[4.49 0.0681 0.0513]
Stator resistance Rs (pu)	0.003

3.4.3 Excitation System and Automatic Voltage Regulator

The excitation system and the automatic voltage regulator were implemented to stabilize the output voltage of the synchronous generator and to dynamically adjust the terminal voltage according to the change in the load. AC5A IEEE system was implemented by using a Matlab/Simulink blocks.

The calculation and control strategy was developed and implemented in the Matlab/Simulink blocks based on the recommendations provided by IEEE for per-unit systems. The voltage regulator will calculate the difference between the reference field voltage for the synchronous generator (Vref) and the measured field voltage (Vt). Then, a controller will be implemented to tune and eliminate the error. Figure 18 shows the internal structure of the excitation and voltage regulator system.

Figure 18 Diesel generator AVR and excitation system model

3.5　　Energy Storage and Control Strategy

3.5.1 Power Management System

Due to the irregularity and fragmentary of the renewable energy sources, which is caused by the variations in solar irradiation levels as well as wind speeds, it is highly doubtful that the AC/DC loads on board of the platforms will be only supplied by the renewable sources. Hence, a control strategy should be applied to regulate different operating conditions involving renewable sources, emergency generator, and energy storage and dumping system. The control strategy should define the power demand needed for the AC/DC loads of the unmanned platform and will apply the best system topology in order to efficiently supply the loads at all time. Also, the controller will be responsible for charging/discharging the battery system as well as running/ disconnecting the emergency diesel generator.

3.5.2 Controller Input and Output data

The proposed control strategy has three inputs, on/off signal to the emergency diesel generator, Battery System State of Charge (SOC), and the amount of power to be dumped. The control strategy working principle is as follow, first, the solar power, wind power, and load demand should be known. Therefore, the controller determines, based on the previous obtained data, if there is an excessive or shortage in power supply in the hybrid system. If there is an excessive amount of generated power, the system will check the SOC for the battery bank. Provided that the SOC for the battery bank is more than 85 %, which means that the battery bank is fully charged, the

excessive power will be treated as a surplus power and will be dumped, otherwise it will be sorted and used to charge the battery bank.

In addition to that, the SOC for the battery bank activates the on/off signal to the generator. If the SOC is less than 20 %, which indicates that the battery bank is depleted, then the emergency diesel generator will be turned on. To ensure a smooth operation for the power system and a continuous non-disturbed supply to the loads, the emergency diesel generator should be turned on before the battery bank is fully depleted.

3.6   Optimization Study

In this section, the optimization study of the hybrid power system is presented. The main objective of the optimization study is to achieve the optimal design of the hybrid system components with the lowest cost. The study is carried out by using HOMER software which is introduced by the American National Renewable Energy Laboratory (NREL) and is dedicated to the optimization studies of off-grid hybrid power systems. Moreover, the study will determine the ratings and sizing of each system components during the lifetime of the project which is estimated to be 20 years (based on the lifespan of PV panels). The general flowchart of the optimization study is shown in Figure 19.
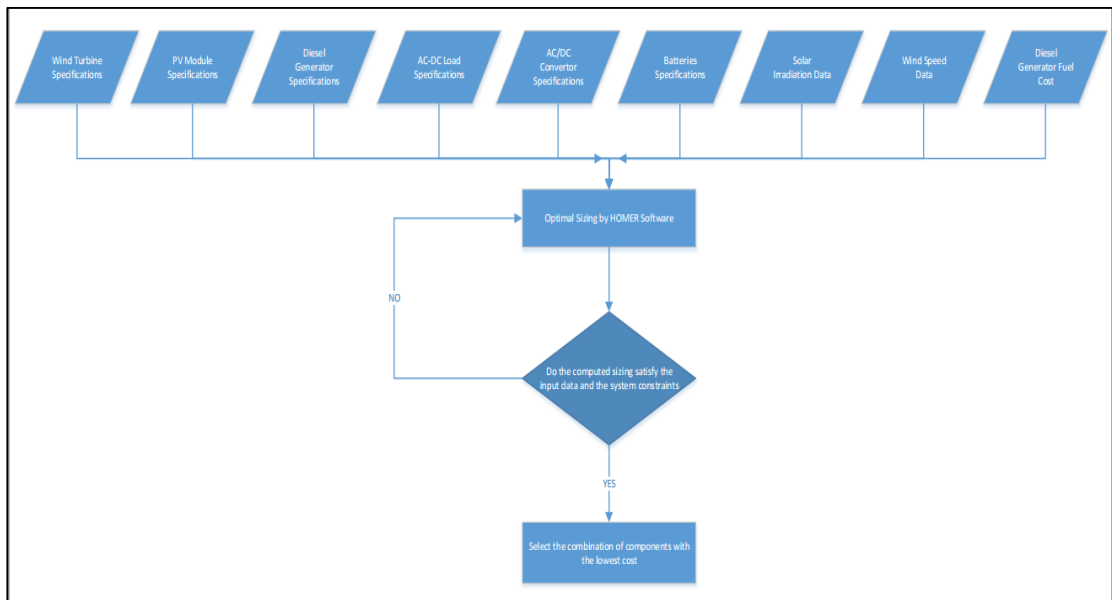
Figure 19 the general flowchart of the optimization model

3.6.1 The proposed optimization technique

The optimization technique selected is a parametric based approach. The optimization model takes inputs from the hybrid system components as well as the wind data, solar data, and diesel generator fuel cost. In addition to that, and seeking for the simplicity of the analysis, the power ratings of the hybrid system components will be fixed. However, the optimization model will vary the number of units for each components, scaled annual irradiation level for the solar data, and scaled annual wind speed for the wind data.

After constructing the hybrid system on HOMER software as shown in Figure 20, the simulation will run for specifying the optimal system components that satisfy the objective function of the optimization study.
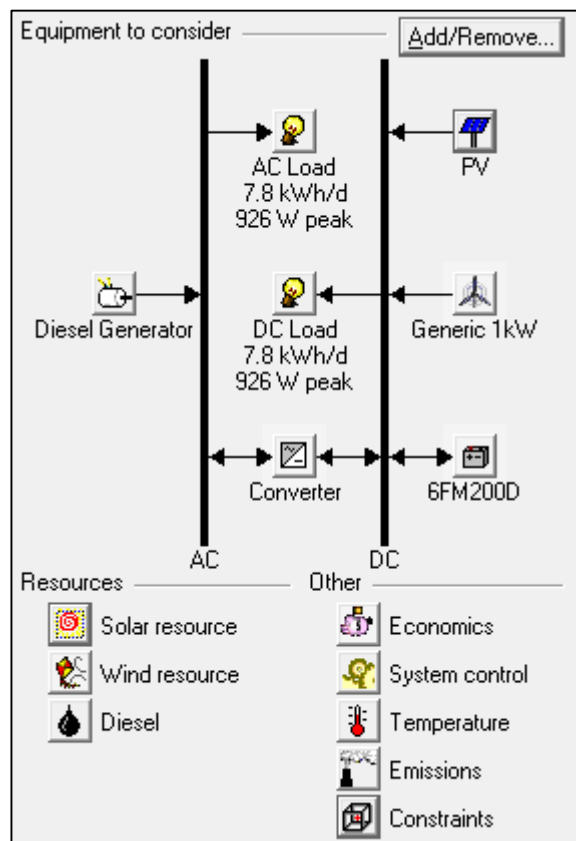
Figure 20 Hybrid power system model in HOMER software

3.6.2 Cost objective function

The objective function of the study is to reduce the total cost of the project during its total lifetime. Lifetime of the project will be considered as the lifetime of the solar photovoltaic modules as they have the longest lifespan amongst all the system components. The cost objective function of the project is represented by the net present

cost (NPC) of the project investment starting from the installation and commissioning cost to a discounted value of operation and maintenance costs and hybrid system components replacement cost. The inflation rate during the project lifetime will also be taken into considerations.

The general equation of the cost objective function which will be used in the optimization model includes capital cost (CC), annual operation and maintenance cost (OMC), battery banks replacement cost ($RC_{Cost-Batteries}$), replacement cost of the solar photovoltaic modules, replacement cost of the wind turbines, and the diesel generator fuel cost (FC). All the cost will be calculated based on the total lifetime of the project. However, the cost for inverters, rectifiers, system cables, and the overall control system of the project will not be taken into considerations because they represent a small share of the total system cost comparing with the major system components mentioned in the first part. Consequently, the general equation of the cost objective function of the project is as follow:

$$OF_{Cost} = CC + OMC + RC_{Cost-Batteries} + RC_{WT} + RC_{PV} + FC \qquad (3.43)$$

Where:

- OF_{Cost} : Total objective function cost.
- CC : Capital cost of the project.
- OMC : Annual operation and maintenance cost.
- $RC_{Cost-Batteries}$: Replacement cost for the battery banks.
- RC_{WT} : Replacement cost for the wind turbines.
- RC_{PV} : Replacement cost for the solar photovoltaic modules.
- FC: Diesel generator fuel cost.

The detailed description of each term of the general equation will be illustrated in the following sections.

Capital cost

The capital investment of the project includes the cost of studies and designs, plant, machinery, installation, and labors work. In this project the capital cost is specifically presented for each major component of the hybrid power system. Also, capital cost is a present cost which indicates the real cost of the project at the starting time of the project. The capital cost (CC) is presented by:

$$CC = P_{Wind} + P_{PV} + Q_{Battery} + P_{Convertor} + VC \qquad (3.44)$$

Where:

- CC : Capital cost.
- P_{Wind}: Wind turbine cost.
- P_{PV}: Solar photovoltaic modules cost.
- $Q_{Battery}$: Battery bank cost.
- $P_{Convertor}$: AC/DC power convertor cost.
- VC : Additional costs.

Operation and maintenance costs (OMC)

The annual operation and maintenance costs includes the maintenance cost of batteries, wind turbines, wind turbines inverters, and solar photovoltaic panels. In addition to that, the labors salaries and maintenance cost of the backup diesel generator will be taken into considerations. The assumption made of the calculation is based on the fact that OMC is almost stable and usually equals to a percentage of the total capital cost of the project (CC). However, the increase of the OMC will only result from the change in the inflation rate (*fr*) as well as the discount rate or the interest rate of the project (*ir*).

$$OMC = OMC_\% * CC * \left(\frac{1+fr}{1+ir}\right)^t \qquad (3.45)$$

Where:

- OMC : Annual operation and maintenance costs.
- $OMC_\%$: Proposed percentage of the annual operation and maintenance costs.
- CC : Capital cost.
- fr: Inflation rate.
- ir : Interest rate.
- t : Project lifetime (years).

Replacement cost of the batteries (RC)

The replacement cost of the batteries identifying the replacement of existing batteries or purchasing of new batteries during the project lifetime as the typical battery lifetime is far less the project lifetime which is assumed to be 20 years. An assumption is made

to specify the replacement cost of the batteries during the project lifetime. The assumption is based on the battery cost is not going to change significantly during the project lifetime and will only be affected by inflation rate. The present value of the battery replacement cost taking into considerations the interest rate.

$$RC_{Batteries} = Q_{Battery} * \frac{1}{(1+ir)^t} \qquad (3.46)$$

Where:

- $RC_{Batteries}$: Battery banks replacement costs.
- $Q_{Battery}$: Battery bank capital cost.
- ir : Interest rate.
- t : Project lifetime (years).

Replacement cost for the solar PV modules and wind turbines:

Assumptions have been made for the replacement of the PV modules as well as the wind turbines in the hybrid system. Theses assumption are based on the long lifespan of the two components which is typically range from 15 to 20 years. Hence, the replacement cost for both components will be assumed as a fixed percentage of the initial capital cost. The replacement cost calculations for PV modules and wind turbines are illustrated by:

$$RC_{PV} = P_{PV} * Fp_1 \qquad (3.47)$$

$$RC_{WT} = P_{WT} * Fp_2 \qquad (3.48)$$

Where:

- RC_{PV} : Replacement cost of solar PV modules.
- RC_{WT} : Replacement cost of wind turbines.
- P_{PV} : Capital cost of PV modules.
- P_{WT} : Capital cost of wind turbines.
- Fp_1 : Fixed percentage for PV.
- Fp_2 : Fixed percentage for Wind turbines.

Fuel cost:

The total cost of the diesel generator fuel is calculated based on varying the fuel cost per liter starting from 0.3 \$/L to 0.6\$ per liter and with an increment of 0.05 \$ per liter

for each simulation trial. The mentioned numbers were selected based on the general equation of the total fuel cost consumed by the diesel generator during the project lifetime taking into considerations the yearly fuel consumption, inflation rate (fr) and interest rate (ir) .

$$FC_t = \sum_{SY}^{LS-1} Fuelconsumption_{Yearly} * FuelCost_{2015} * (\frac{1+fr_{fuel}}{1+ir}) \qquad (3.49)$$

Where:

- FC_t : Total fuel cost during the project lifetime.
- $Fuelconsumption_{Yearly}$: Yearly fuel consumption rate.
- $FuelCost_{2015}$: Average fuel cost for the project starting year (2015).
- fr_{fuel} : Inflation rate for fuel price.
- ir : Interest rate.
- LS : Project lifespan (years).
- SY: Project starting year (SY=1).

3.7 Key Milestone

No.	Item/Week	1	2	3	4	5	6	7	8	9	10	11	12	13	14
1	Solar Photovoltaic Models	■	■	■	■										
2	Diesel Generator Modelling and Simulation					■	■								
3	Energy Storage System and General Control Strategy							■	■	■					
4	Optimization Study										■	■	■	■	

3.8   Gantt Chart

No.	Item/Week	1	2	3	4	5	6	7	8	9	10	11	12	13	14
1	Project Methodology	■													
2	Extended Literature Review		■	■	■	■									
	Preparing Progress Report						■								
3	Progress Report							■	■						
4	Pre-SEDEX									■	■				
5	Preparing Final Dissertation & Technical Paper											■	■		
6	Preparing for Viva													■	■

CHAPTER 4 : RESULTS AND DISCUSSION

4.1   Hybrid System Feasibility Study

Project Location

The project location is selected to be 120 km form the shores of Sabah and Sarawak state and in line with Bintulu City. The coordination of the selected location are: Longitude: 4.088 latitude: 112.567. Figure 21 shows the proposed project location.
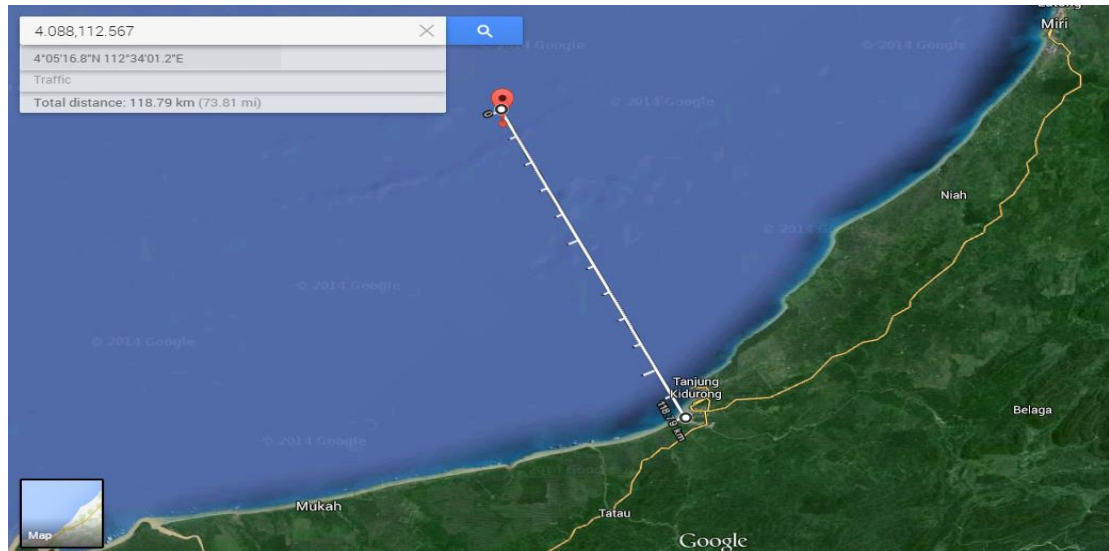
Figure 21 Project location map (Southeast China sea)

Ambient Temperature Profile at Southeast China Sea

The monthly average temperature profile data was obtained by using the database for NASA Surface Meteorology and Solar Energy. The database was gathered and analysed over 22 years by using several satellites for data collection and analysis. In Figure 22, maximum, minimum, and average monthly temperature profile is presented. Moreover, analysing the temperature profile of the project location will determine the hybrid system topology that will be used in the project.
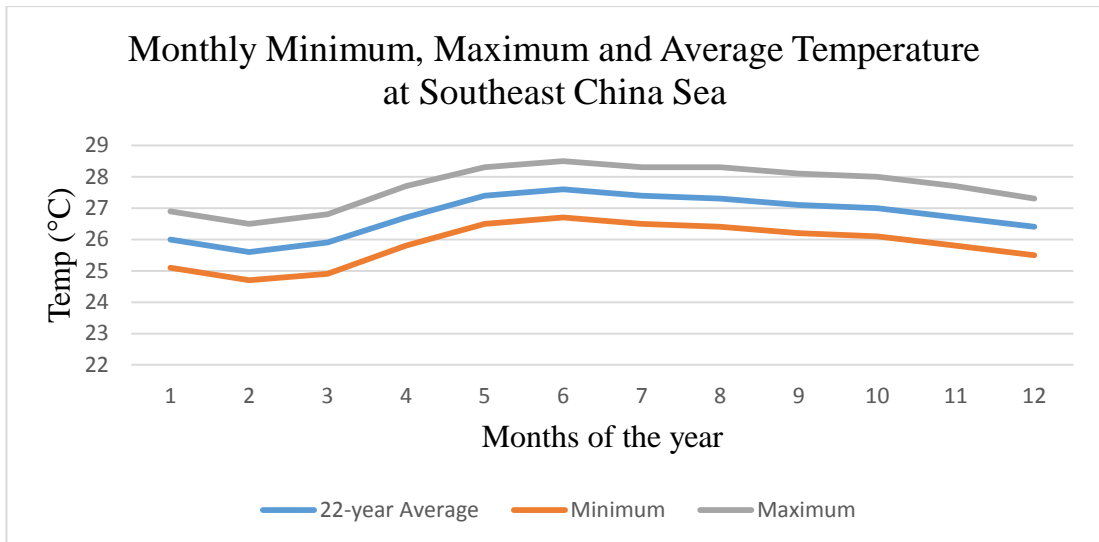
Figure 22 Temperature profile at Southeast China sea

Solar Irradiation and Daylight Hours at Southeast China sea

The monthly average solar irradiation and daylight hours are presented in Figure 23 to determine the potential of solar energy and the amount of power that can be generated by utilizing solar panels. Also, NASA Surface Meteorology and Solar Energy database will help the author in identifying the parameters of a photovoltaic panels, average daylight hours per month and battery sizing and capacitance for the photovoltaic panels to ensure continuous supply of power during no-sun days.
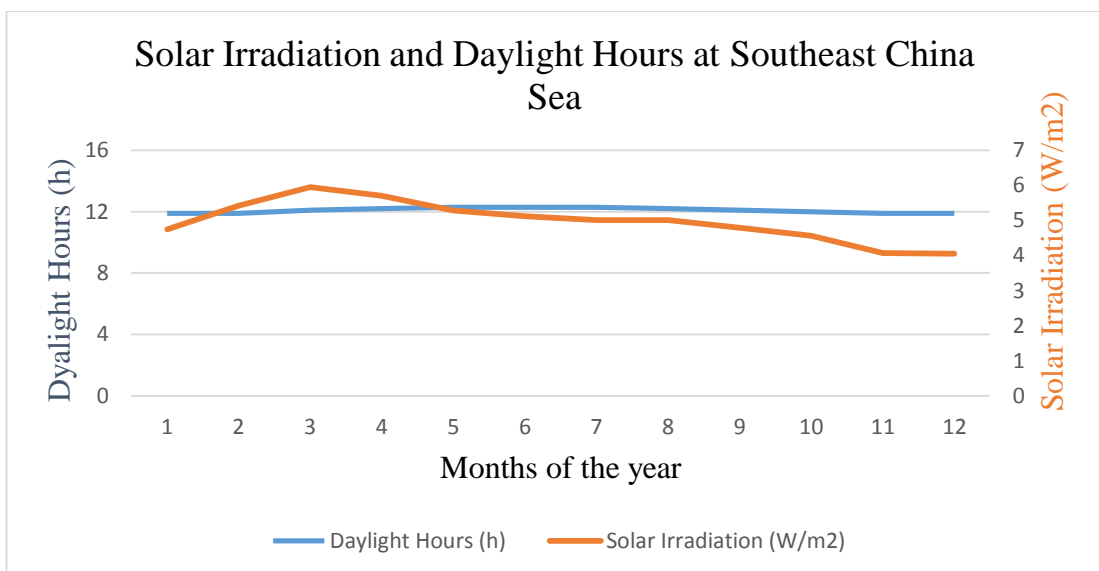
Figure 23 Hours of daylight-solar irradiation at Southeast China sea

Wind Profile at Southeast China Sea

One of the most important key points of the feasibility study is to identify the wind profile and solar irradiation levels in the selected region. Moreover, the analysis of both profiles will determine the total electrical power production of the system. In

Figure 24, solar irradiation and wind speed profiles are presented. It can be shown that wind speed profile does not have a regular patterns just like the solar irradiance profile. Hence, both solar energy and wind energy will be considered for the project to achieve the best result regarding the total power generated from the system.
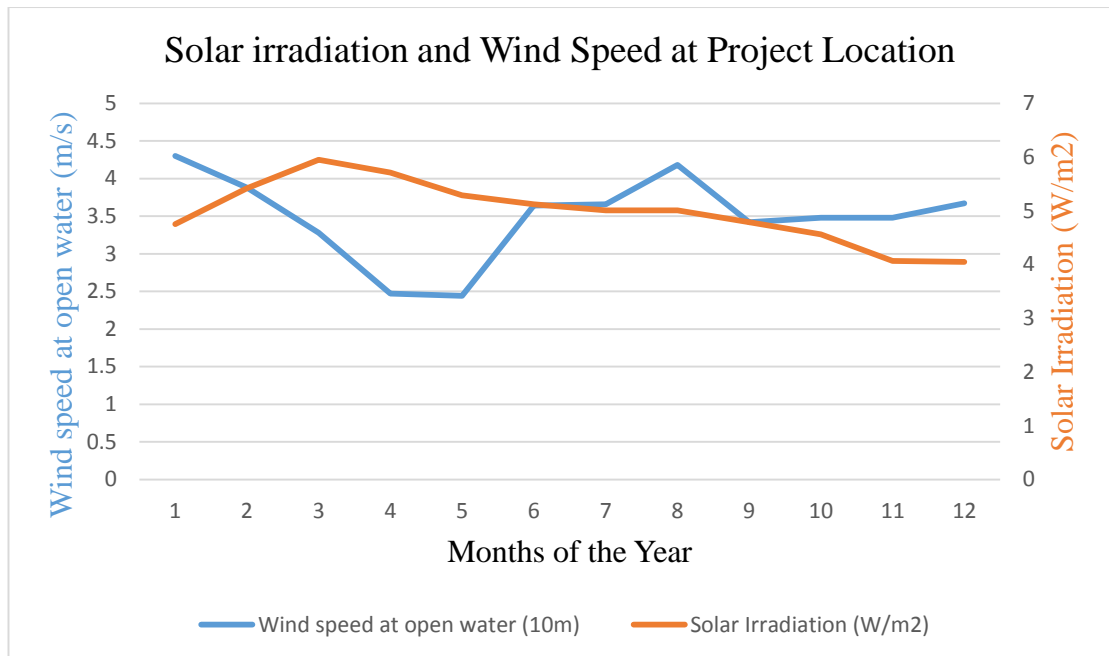
Figure 24 Solar irradiation and wind speed profiles at Southeast China sea

4.2   Solar Photovoltaic Models

4.2.1 The First Model

Simpowersystems™ block representation were used to implement the mathematical equations described in section 4.2 of the methodology. Integration between the mathematical model and the power system model is achieved and the simulation was applied in no-load environment. The detailed model is illustrated in Figure 25.
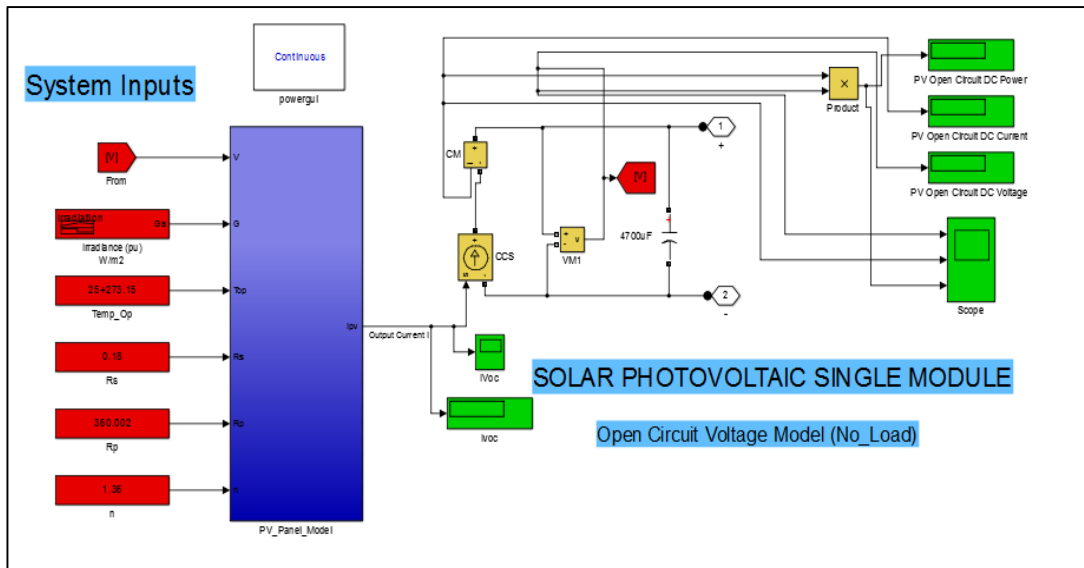
Figure 25 The First solar photovoltaic model

The solar photovoltaic module was built based on the manufacturer datasheet of Solarex-MSX60 60Wp Solar Module. The module output voltage depends on the variations in solar irradiance levels (Ir) as well as the operating temperature (Top). No load I-V graphs were created by simulating the first model with various irradiation levels as well as various operating temperatures and the graphs characteristics are shown in Figures 26 and 27 respectively.
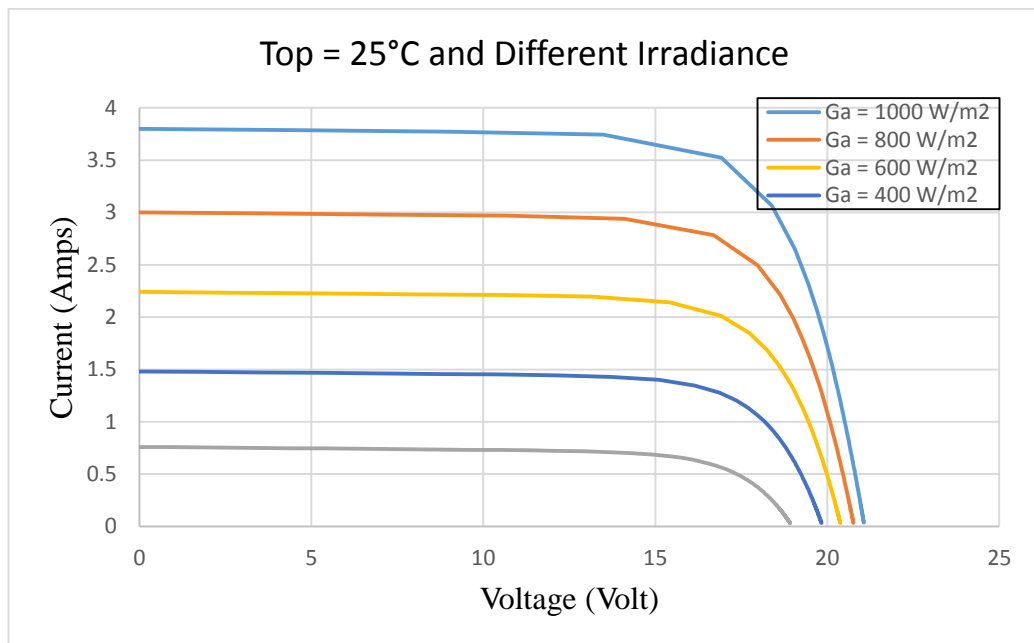
Figure 26 I-V curve with fixed operating temperature and different irradiation
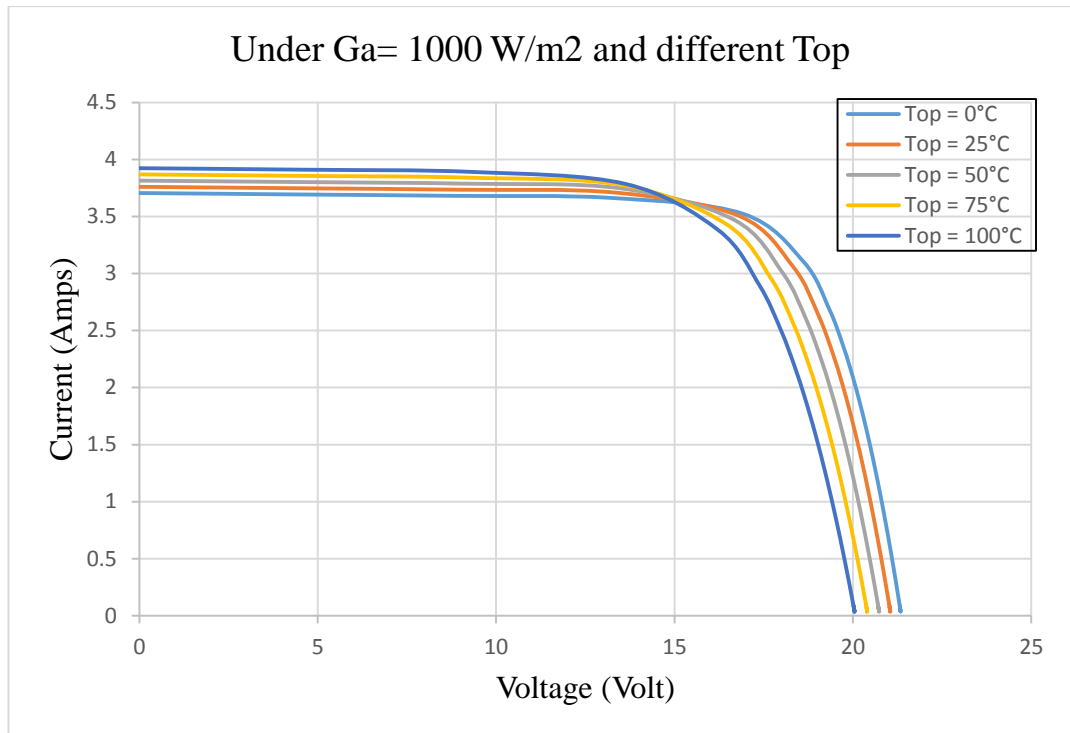
Figure 27 I-V curve with fixed irradiation and different operating temperatures

4.2.2 The Second Model

The second model was built and simulated in Matlab/Simulink environment to attach an output variable resistance to the single solar photovoltaic module implemented in the first model. The second model is presented in Figure 28. Moreover, a ramp function was used to vary the value of the resistance and the output results are obtained in Figure 29. The resistance value used in the second model was 5.2 ohms and the ramp function slope was 2.5 with zero start time.
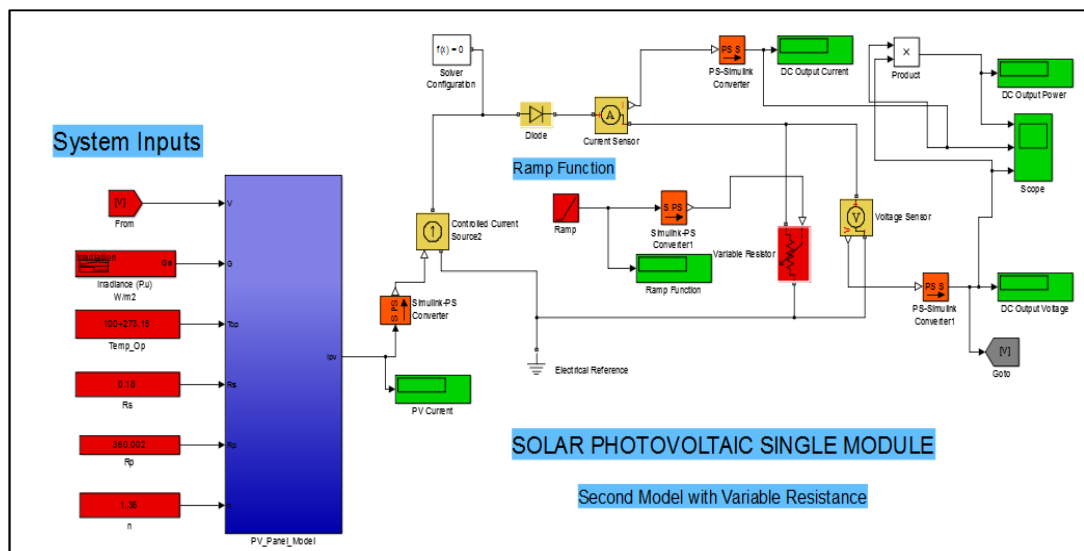
Figure 28 The second model for a single solar photovolrtaic module
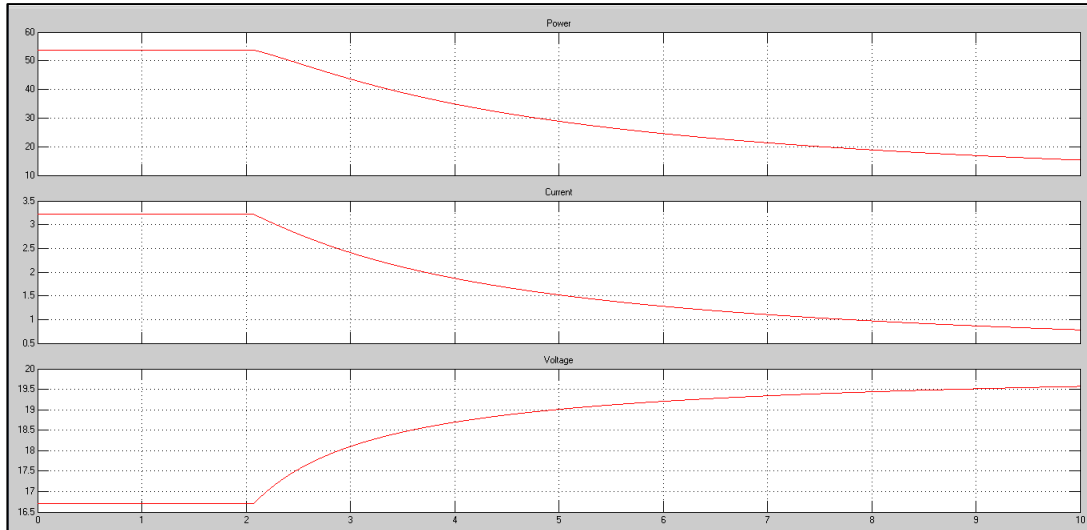
Figure 29 Power, current, and voltage output values for the second model

4.2.3 The Third Model-Buck Convertor and MPPT Controller

The third model was implemented to control the solar array system output voltage regardless of the values of the load resistance. The model schematic is shown in Figure 30. The third model is constructed of a solar photovoltaic system of 2 parallel arrays with 10 series modules in each array. The maximum output power Pmpp from the system is calculated to be 1100 watts according to Solarex-MSX60 60Wp Solar Module characteristics used in the model.
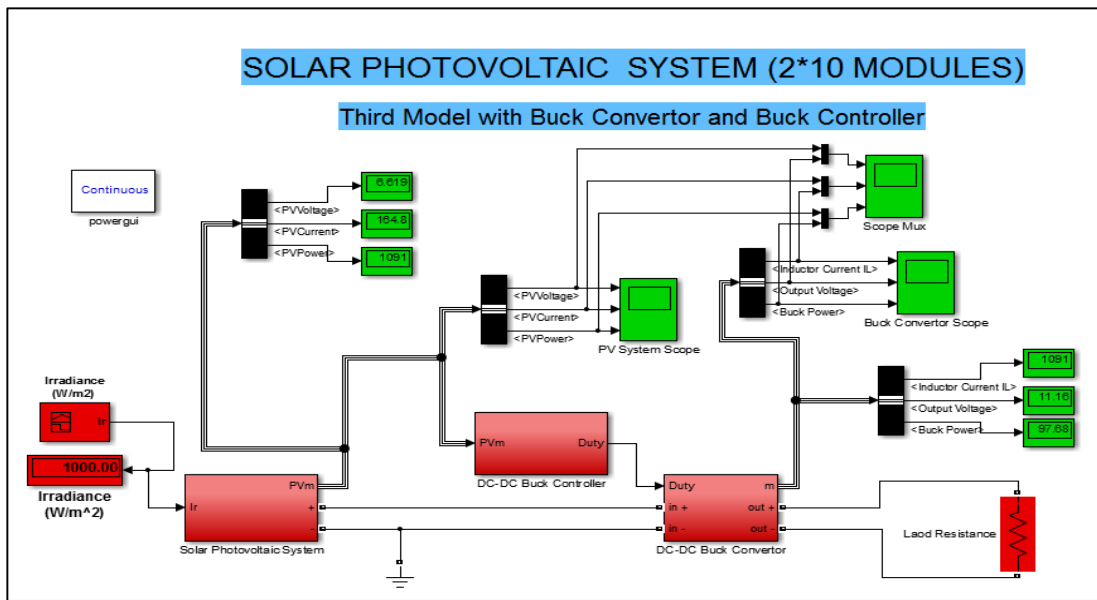
Figure 30 The third model with buck convertor and controller

The model was tested in standard conditions; irradiation level of 1000 w/m2 and operating temperature of 25° C, and the module values was obtained from the first and second models. The internal structure of each block diagram in the third model is

48

illustrated in Figures 31, 32 and 33 respectively. In Figure 31, the PV array and PV single module are presented. A smoothing capacitor of 1200 uf was added to the reference PV single module to filter the output voltage signal which is going to be used as an input value to the controller.
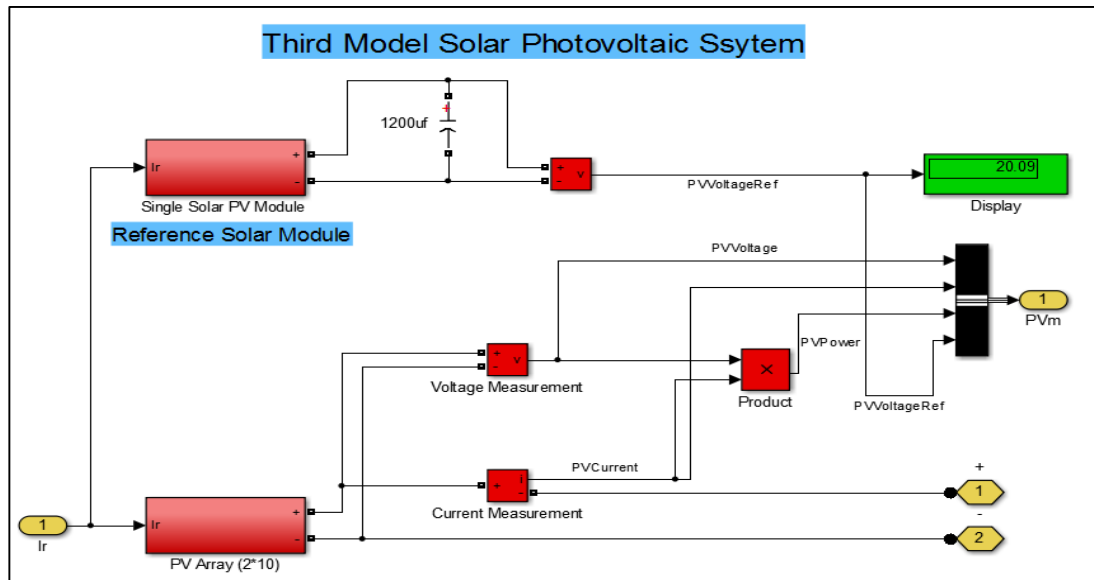
Figure 31 Solar photovoltaic system schematics
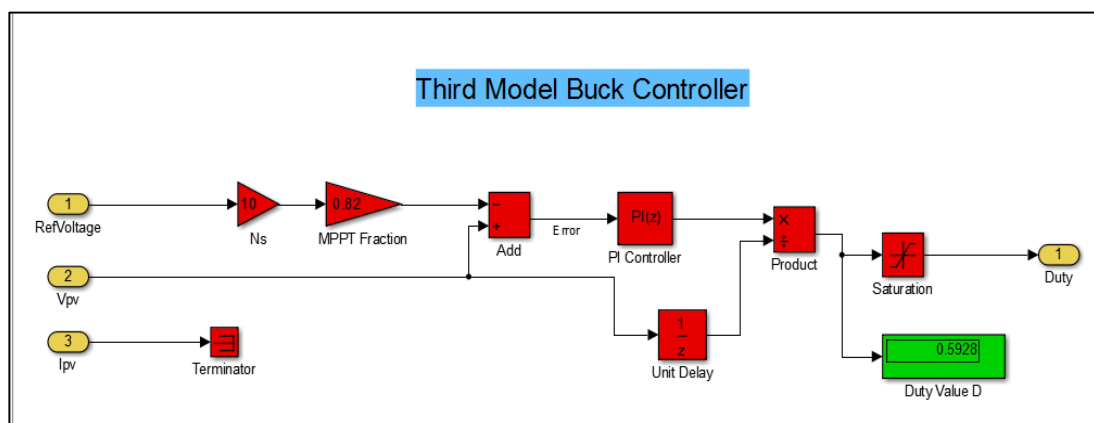
Figure 32 Fractional open-circuit voltage MPPT algorithm

In Figure 32, the MPPT algorithm and the controller is used to dynamically adjust the switching frequency of the buck convertor. PI controller gains used in the model are $Kp = 10$, $Ki = 5$. Moreover, the fractional value K used in the algorithm is 0.73 for Solarex-MSX60 60Wp Solar Module.
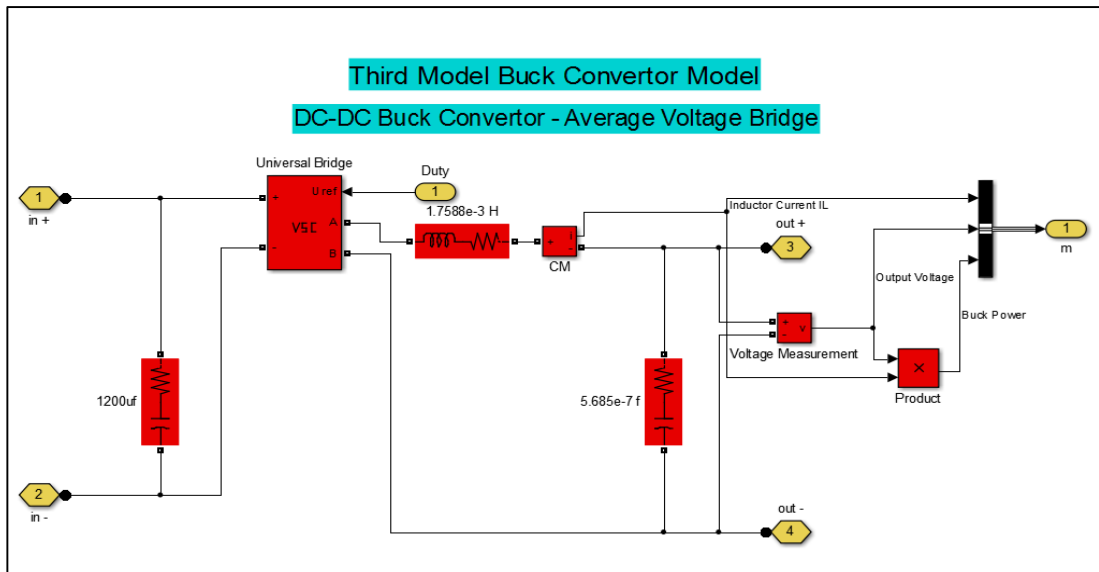
Figure 33 Buck convertor Simulation blocks

In Figure 33, a voltage source convertor (VSC) is used to control the output voltage. The convertor is being switched by the controller. The values used for the buck convertor are illustrated in Table 6.

Table 6 Buck convertor parameters

Parameter	Value
Vin	$171 Volt$
Po	$1100 Watt$
D	0.6
Io	$11.6 Amps$
L	$1.7 mH$
C	$0.56 uf$

Based on the calculations, the buck convertor input voltage and input current are 170 V and 6.5 A respectively. Hence, the output voltage and current are 100 V and 11.6 A respectively.
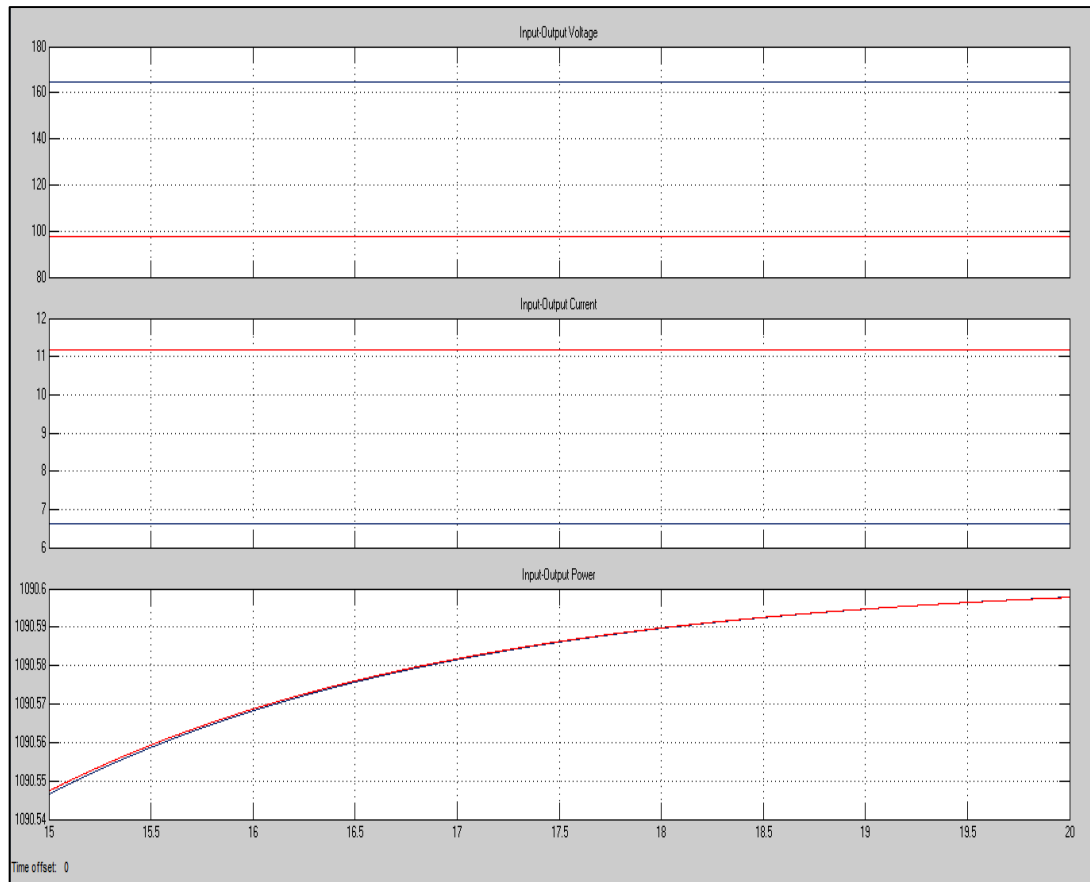
Figure 34 Input-output values for the buck convertor

In Figure 34, the final Input-Output values for the buck convertor are shown. The inputs for the convertor are the solar photovoltaic system (Generation side) and the output values represents the output resistance (load side). The maximum output power produced by the photovoltaic array will be maintained despite the changes in the load value. Also, the convertor will step down the output voltage form 170 V in the input side to 100 V on the load side and hence the output current will increase from 6.5 A on the input side to 11.6 A on the output side.

4.3   Wind Turbine Model

The simulated model consisted of:

- Wind Turbine Rotor Blades Aeronautics Block.
- Two-mass Mechanical Drivetrain Block.
- Permanent Magnet Synchronous Generator Block.
- Universal Bridge (Rectifier Circuit) Block.
- Voltage Regulator Circuit Block.

The full model can be seen in Figures 35 and 36.

51
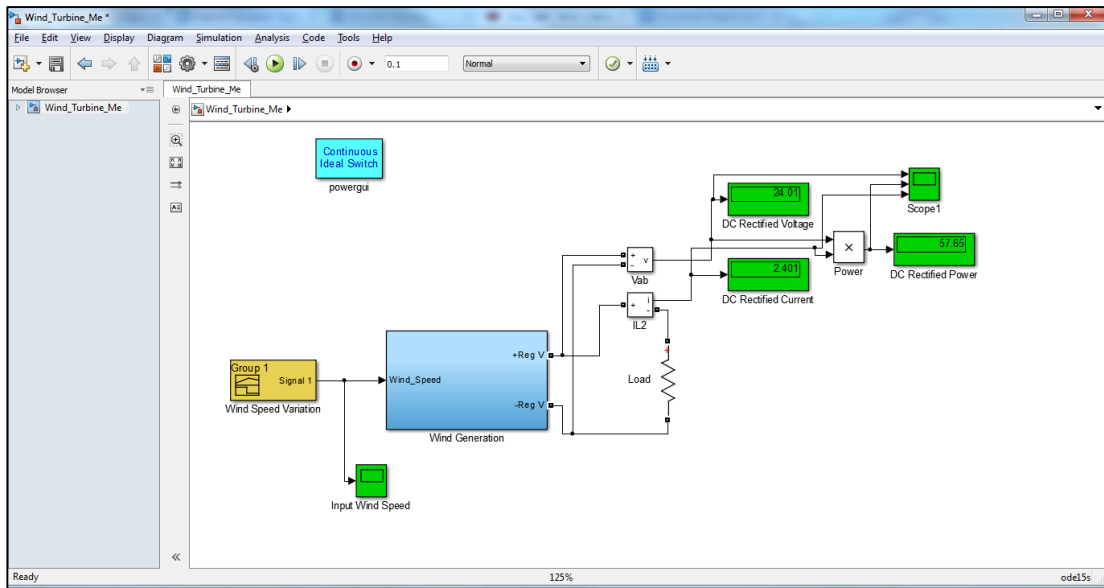
Figure 35 Wind turbine model
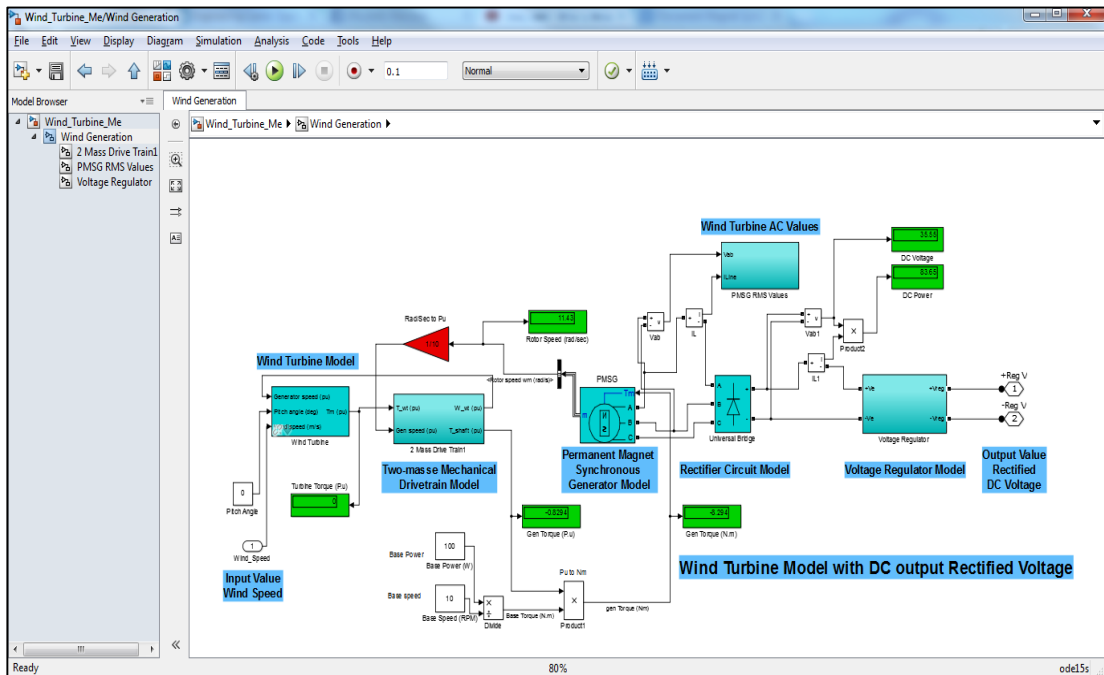
Figure 36 Internal structure of the wind turbine model

4.3.1 Wind Turbine Rotor Blades Aeronautics Block

The model was structured in the Matlab/Simulink environment and it can be used to simulate the effect of wind speed variations on wind turbine output power as shown in Figure 37. Also, the aeronautic block is used to calculate the output torque from the wind turbine blades which will result in an input torque to the mechanical drivetrain model.

52
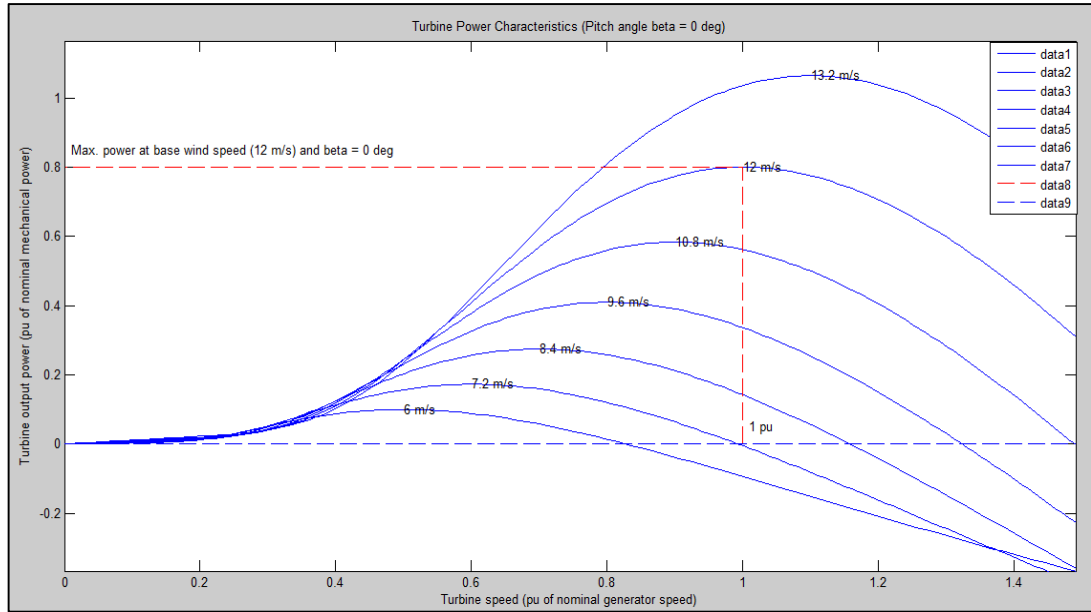
Figure 37 Wind turbine power characteristics (pitch angle = 0)

4.3.2 Two-mass Mechanical Drivetrain Block

The block is used to transform the output torque obtained from the wind turbine rotor to input torque for the synchronous generator. As illustrated in Figure 38, the block utilizes the speed difference between the turbine rotor shaft (slower) and the generator rotor shaft (faster) and hence increase the input torque to the synchronous generator to ensure efficiency and reliability.
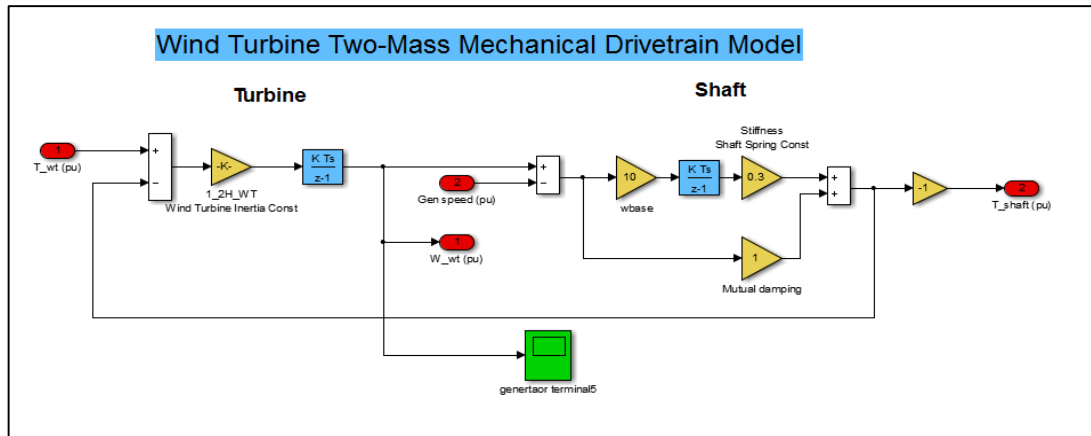
Figure 38 Two-mass mechanical drivetrain model

4.3.3 Permanent Magnet Synchronous Generator Block

The block is used to simulate a synchronous machine with torque as its input value and three-phase AC voltage as the output from the generator. The obtained results are shown in Figure 39. The values indicate the voltage, current and power generated by the synchronous machine.
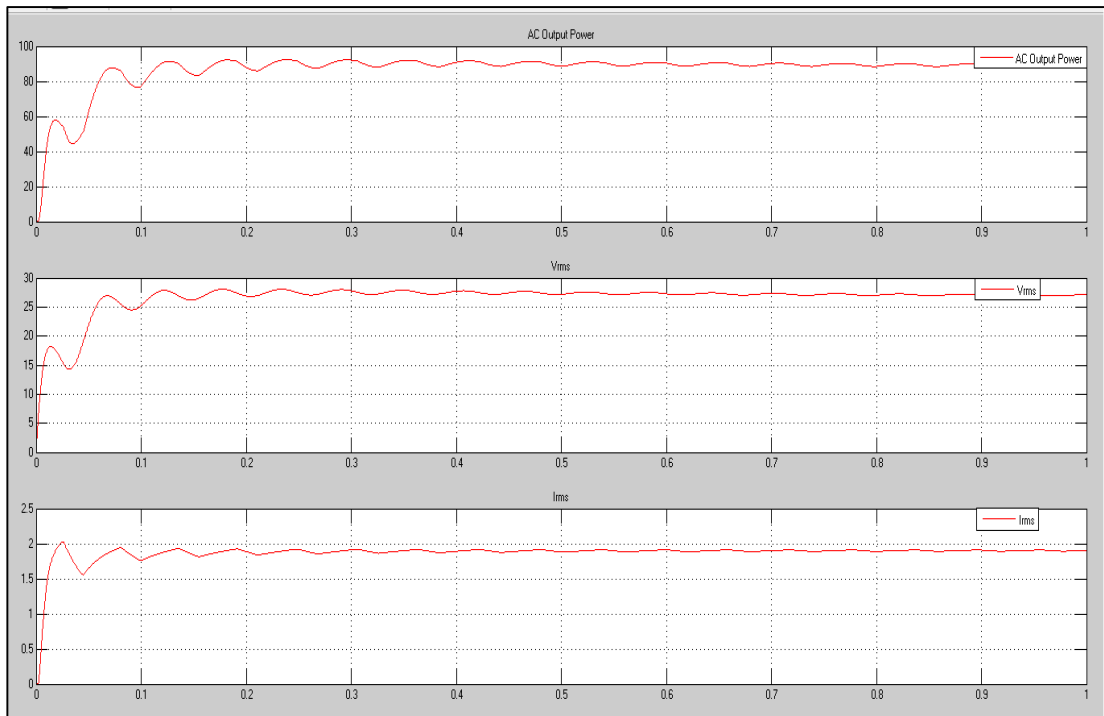
Figure 39 Permanent magnet synchronous generator output values

4.3.4 Universal Bridge (Rectifier Circuit) Block

A universal bridge block was added as an AC-DC convertor for the output voltage of the synchronous machine. The full-wave convertor implements ideal diodes as the main switching devices. The results of the rectified voltage, current, and power values are shown in Figure 40.
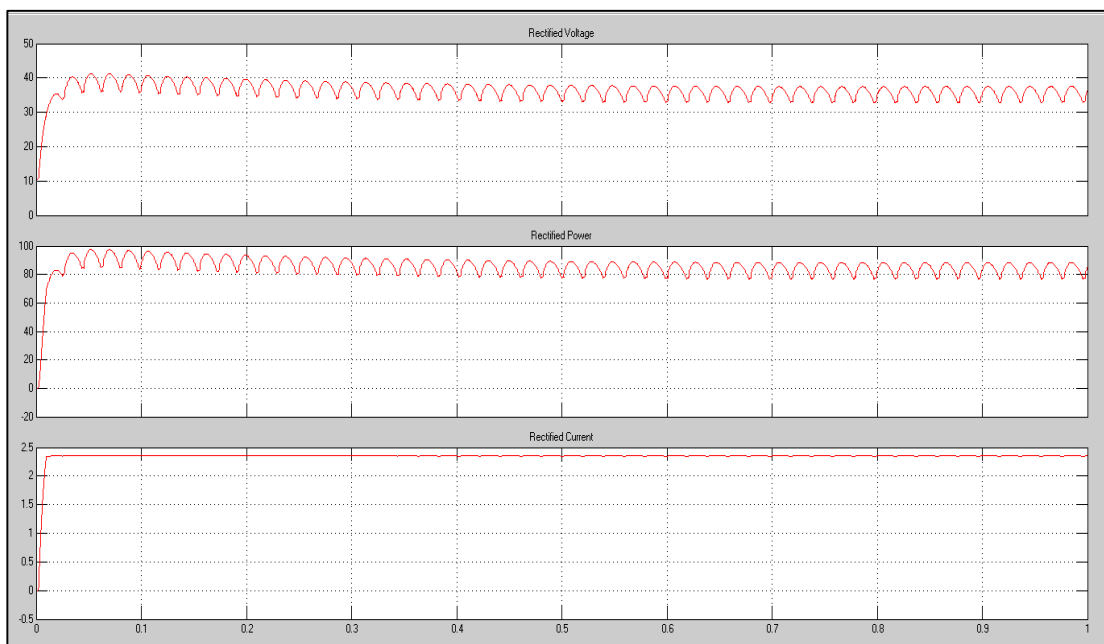
Figure 40 The Rectified values of synchrnous generator output values

4.3.5 Voltage Regulator Circuit Block

Voltage regulator circuit block was implemented to regulate the DC output voltage from the rectifier circuit into 24VDC as the most common DC supply voltage for instrumentation and control devices. The voltage regulator circuit consists of Zener diode, NPN Transistor to control the switching, Op-amp amplifier to control the transistor switching signals and two resistance in parallel to control the output voltage value according to the formula:

$$Vout = V_{Breakdown} * \frac{R_1 + R_2}{R_2} \qquad (5.3.5.1)$$

Where:

- R_1: The first resistor value
- R_1: The second resistor value
- $V_{Breakdown}$: Zener Diode breakdown voltage value

The voltage regulator block used in the simulation is shown in Figure 41. The output regulated values for voltage, current and power are concluded in Figure 42.
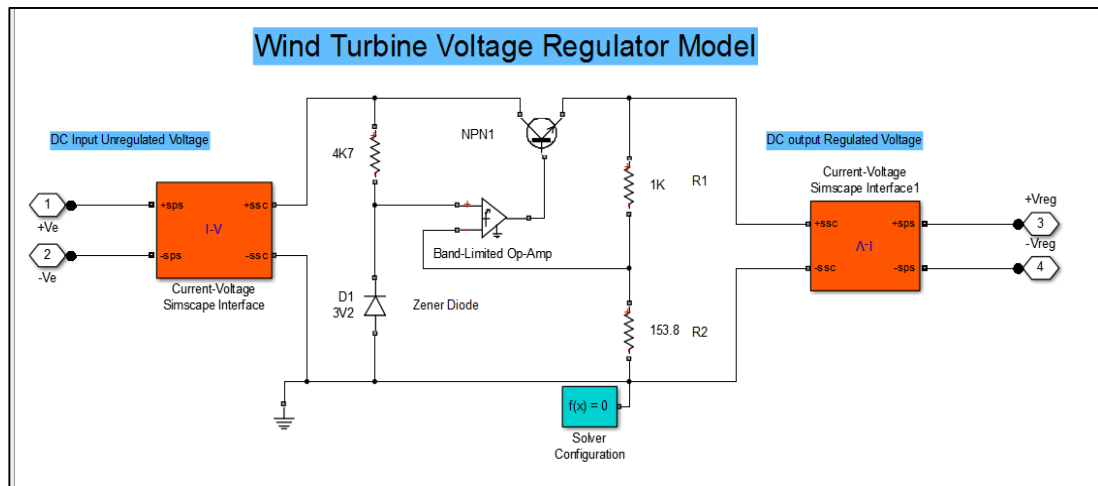
Figure 41 Wind turbine voltage regulator block
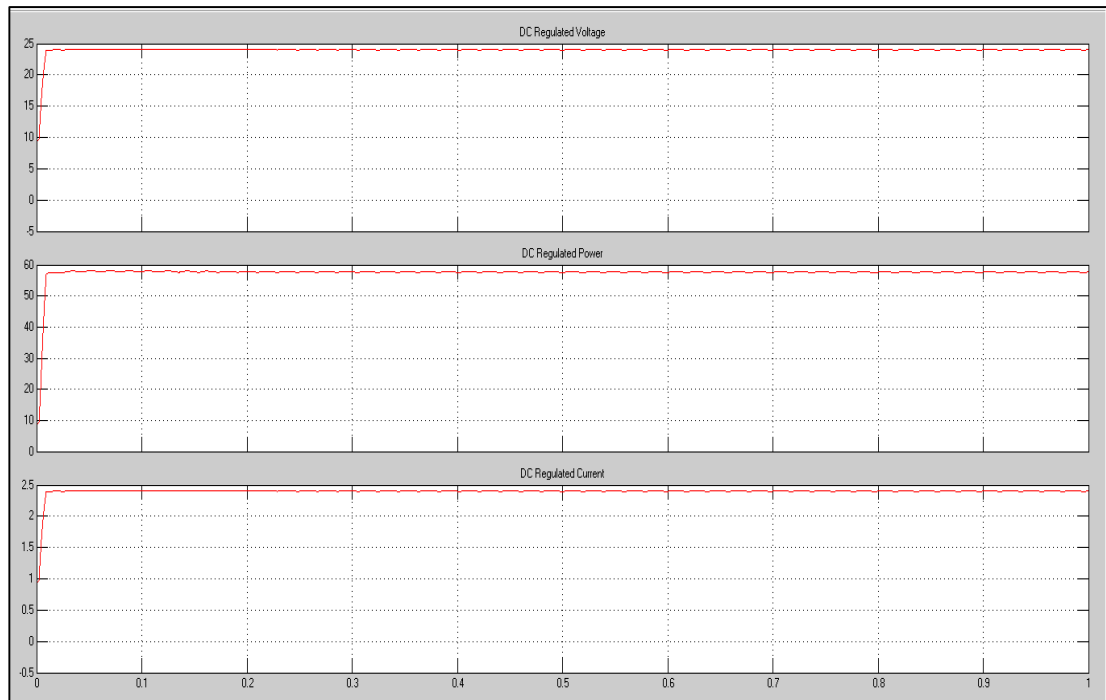
Figure 42 Regulated values of the wind turbine model

4.4 Diesel Generator

The diesel generator modelling and simulation process was achieved using Matlab/Simulink software. The simulation has been implemented to analyze the performance of the diesel generator and the contribution of the excitation system, the speed governor, and the automatic voltage regulator towards increasing the performance and reliability of the system. The diesel generator model showed high stability and reliability while varying the output loads. Moreover, the final control parameters were achieved to stabilize the system output voltage as well as the output electrical active power which will be supplied to the load.

In addition to that, the speed, output voltage, generator field voltage, and output active power waveforms were captured and the performance of the generator was stable during the simulation process. The complete model of the diesel generator is shown in Figures 43,44,45,46 and 47.

56
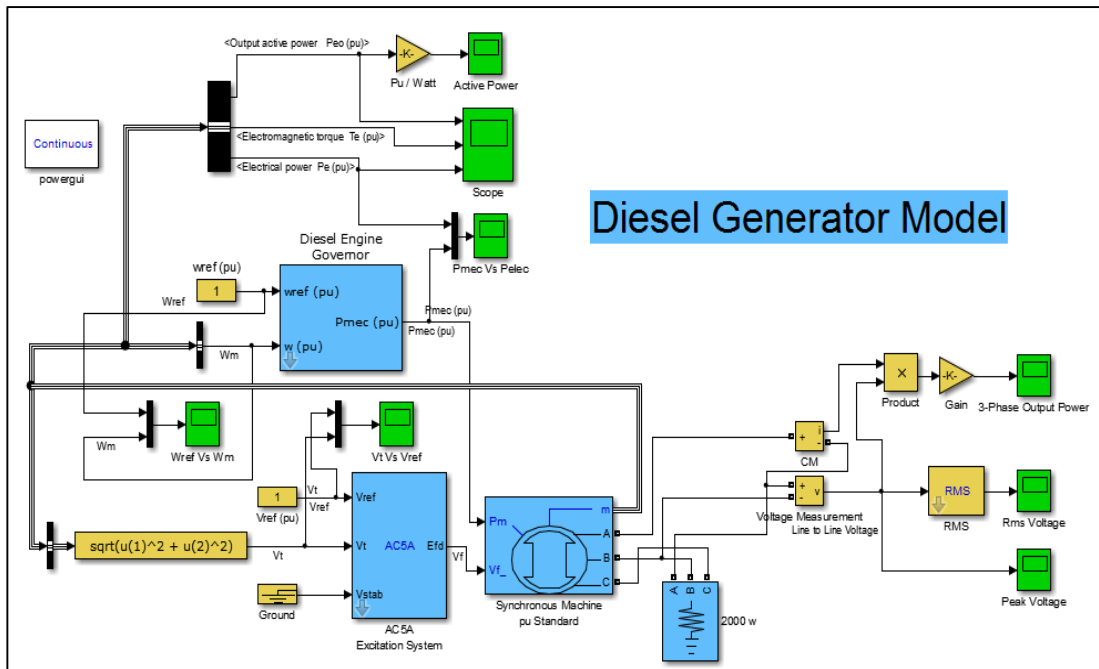
Figure 43 Diesel generator Simulink model
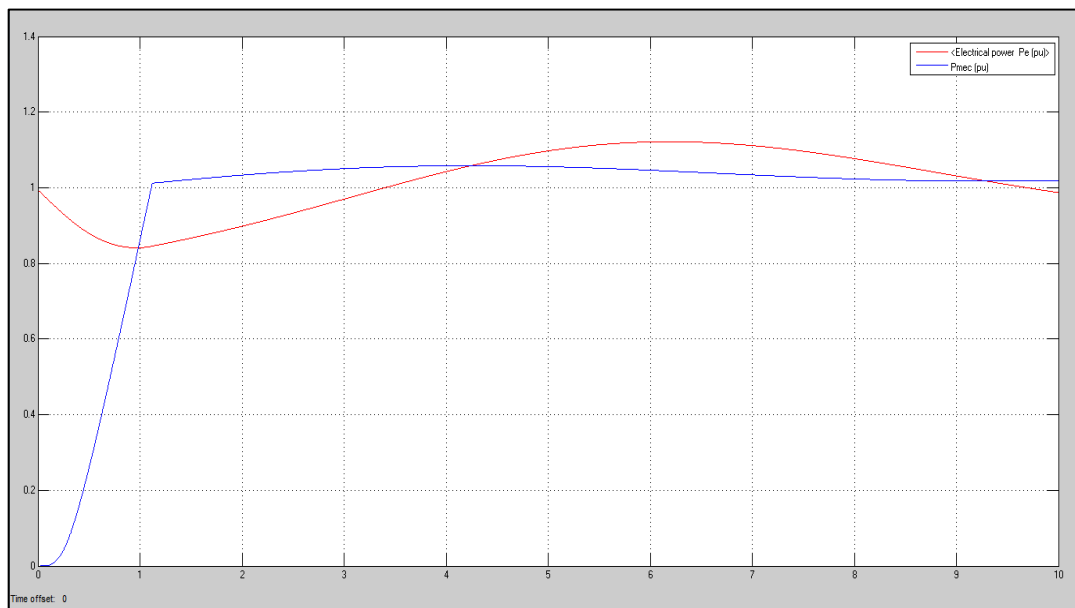
Figure 44 Mechanical vs electrical output power of the diesel generator
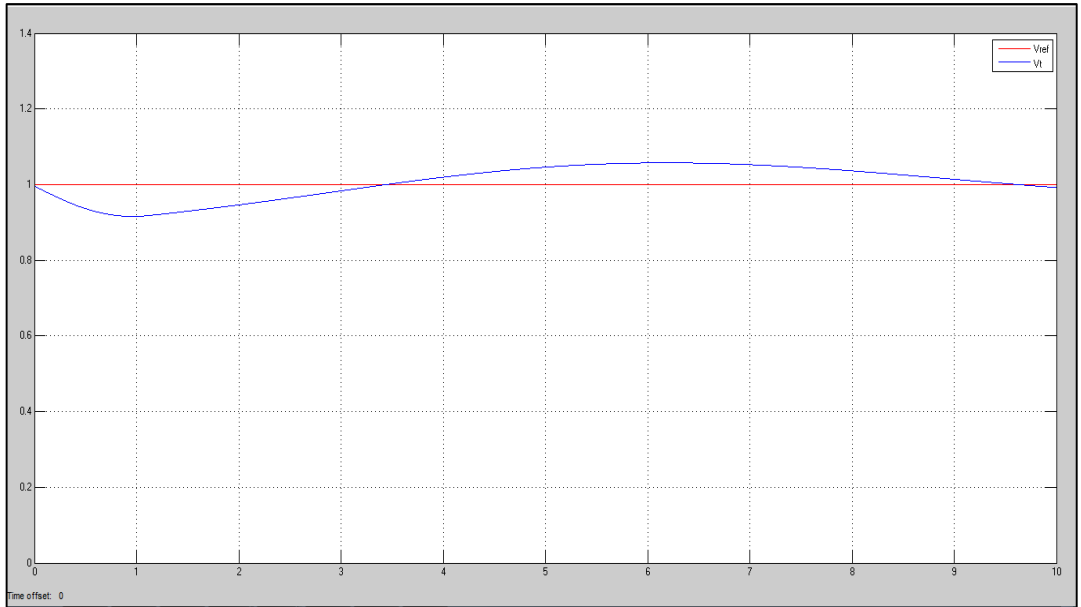
Figure 45 Reference voltage (Vref) vs field voltage (Vf) for the synchronous generator
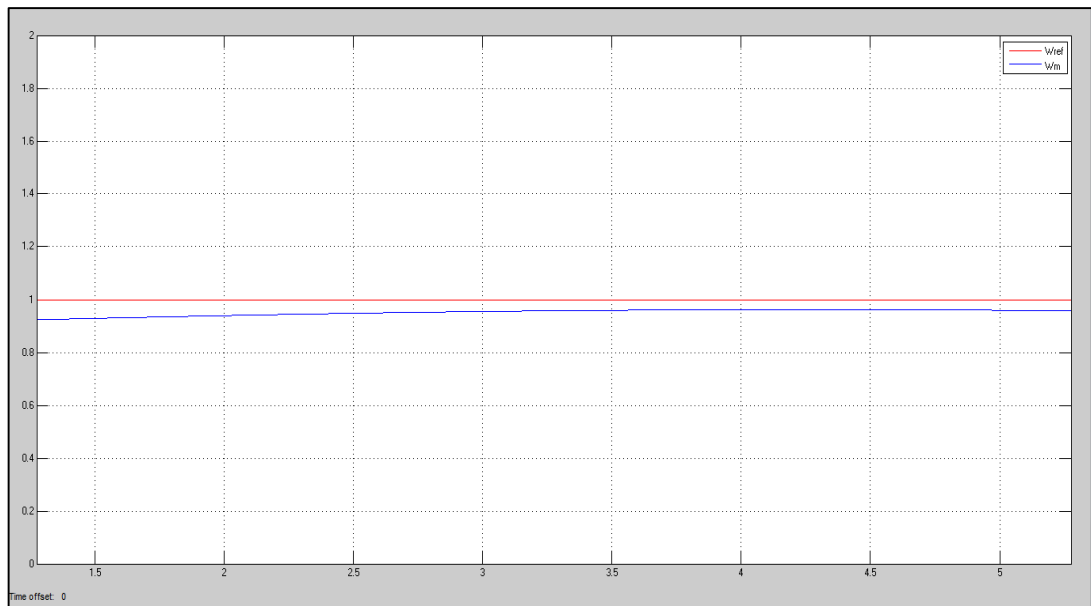
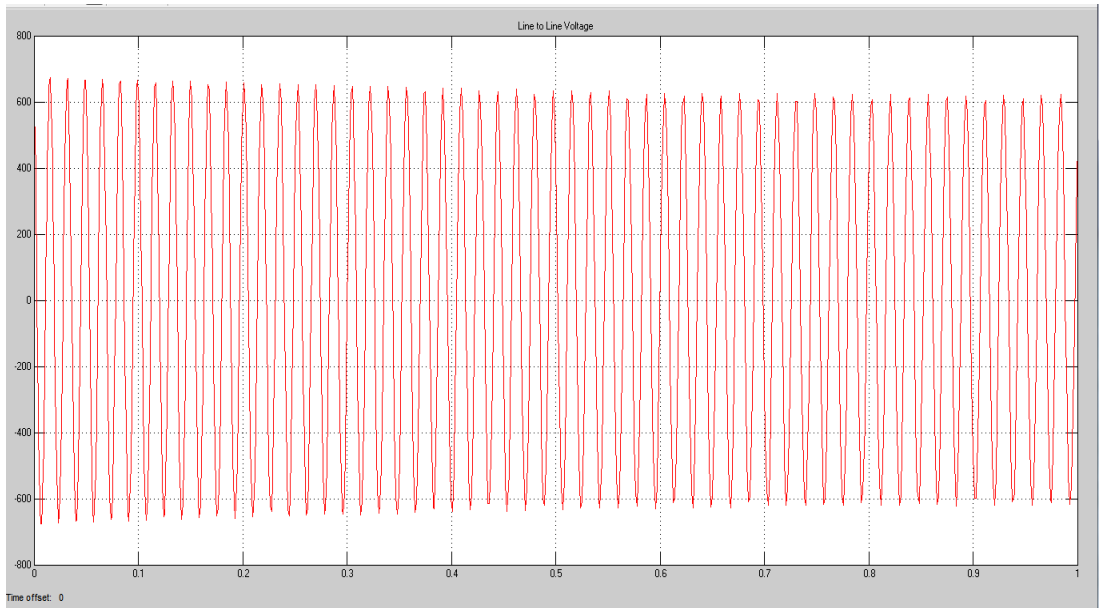Figure 46 Reference speed (Wref) vs adjusted speed (Wm)

Figure 47 Synchronous Generator Output Voltage

4.5   Optimization Study

Prior to running the simulation on HOMER software, the parameters of the hybrid power system components were inserted. Furthermore, wind speed profiles, solar irradiation levels and diesel prices were added to present the actual meteorological data of the project location. In addition to that, the total cost (CC) parameters were calculated and the results were simulated along with the optimization model to achieve the optimal design and sizing for the hybrid system. In Table 7, the solar PV module parameters are listed. The parameters will be used for the optimization study of the system.

Table 7 Solar PV optimization parameters

Module rated power (watt)	300 W
Module lifetime (years)	20 years
Module efficiency (%)	13 %
Module capital cost ($)	500 $
Module replacement cost ($)	400 $
Module OMC ($)	0 $
Number of modules for the simulation	1-10 units
Nominal operating temperature (°C)	25° C
Fixed percentage of replacement (%)	0.0112 %
Average annual irradiation level (Kwh/m^2/d)	4.97 (Kwh/m^2/d)
Project latitude	4.008
Project longitude	112.567

Table 8 shows the wind turbine parameters used in the optimization model. The wind turbine used is a 1 kW horizontal axis Future Energy wind turbine.

Table 8 Wind turbine optimization parameters

Manufacturer	Future Energy
Turbine model	AF1-24v-0125 (406 PMG)
Turbine Blades	3 blades
Startup Wind Speed	2 m/s
Charging Initiation Wind Speed	3 m/s
Rated power (Kw)	1 Kw DC
Lifetime (years)	15 years
Capital cost ($)	3000 $
Replacement cost ($)	2500 $
OMC ($)	50 $
Number of modules for the simulation	1-3 units
Fixed percentage of replacement (%)	0.0112 %
Hub height (m)	6 m
Annual average wind speed (m/s)	4.5 m/s
Project latitude	4.008
Project longitude	112.567

The diesel generator parameters are shown in Table 9. The diesel generator will be utilized in the project as a backup generation set and the renewable fraction of generation will depend on the diesel fuel price as well as the metrological data.

Table 9 Diesel generator optimization parameters

Rated power (Kw)	1 Kw AC
Lifetime (operating hours)	15000
Capital cost ($)	1500 $
Replacement cost ($)	1200 $
OMC ($/hr)	0.05 $
Number of modules for the simulation	1-2 units
Fixed percentage of replacement (%)	0.0112 %
Maximum load ratio (%)	30 %
Generator fuel	Diesel
Carbon monoxide emission factor (g/l)	6.5
Diesel Price ($/L)	0.35-0.6 ($/L)

In Table 10, the battery bank and AC/DC convertor parameters are listed. Battery bank used in the optimization model is Vision 6FM200D and the detailed characteristics are mentioned below.

Table 10 Battery and convertor optimization parameters

Battery nominal voltage (V)	12 V
Battery nominal capacity (Ah)	200 Ah (2.4 kWh)
Battery lifetime throughput (kWh)	917 kWh
Battery capital cost ($)	250 $
Battery replacement cost ($)	200 $
Battery OMC ($)	20 $
Number of battery modules for the optimization	1-12 units
Fixed percentage of replacement (%)	1 %
Convertor rated power (kW)	1 kW
Number of convertor modules for the optimization	1-3 units
Convertor capital cost ($)	1000 $
Convertor replacement cost ($)	1000 $
Convertor OMC ($)	100 $
Convertor lifetime (years)	15 years
Convertor efficiency	85-90 %

The optimization model results are shown in Figure 48 where the complete hybrid power system schematic and the optimal system components are presented.
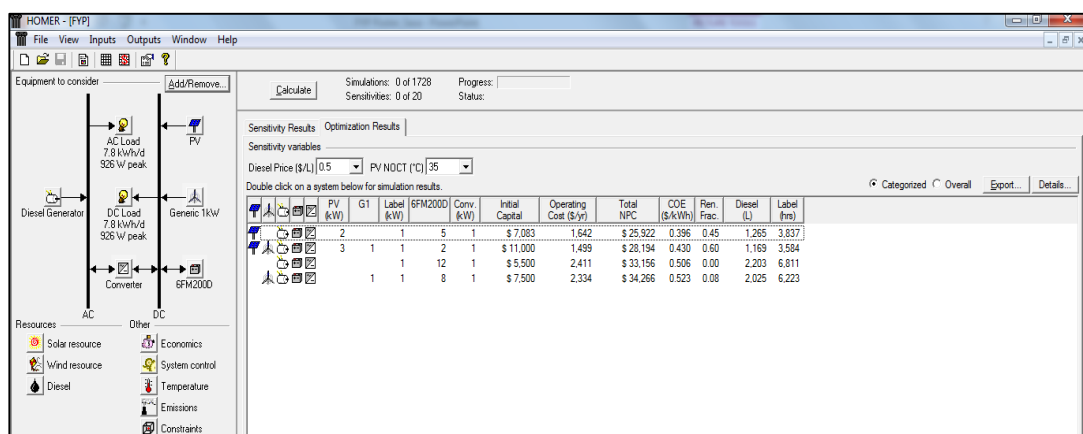
Figure 48 Optimization model results

In Figure 49, a detailed look on the proposed optimal system components is presented. It can be seen that there are four proposed designs for the system which fulfill the cost objective function. However, the first proposed design is the most optimum design for

the hybrid power system in terms of cost reduction. Despite the increase in the renewable fraction of the second design to 60 %, the first design is proved to be the lowest cost with a renewable fraction of 45 %.
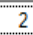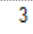
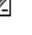|	PV (kW)	G1	Label (kW)	6FM200D	Conv. (kW)	Initial Capital	Operating Cost ($/yr)	Total NPC	COE ($/kWh)	Ren. Frac.	Diesel (L)	Label (hrs)
	2	1		5	1	$ 7,083	1,642	$ 25,922	0.396	0.45	1,265	3,837
	3	1	1	2	1	$ 11,000	1,499	$ 28,194	0.430	0.60	1,169	3,584
			1	12	1	$ 5,500	2,411	$ 33,156	0.506	0.00	2,203	6,811
		1	1	8	1	$ 7,500	2,334	$ 34,266	0.523	0.08	2,025	6,223

Figure 49 Optimal hybrid power system components

The detailed cash flow for the optimum design is shown in Table 11. PV-diesel hybrid power system achieves the best results for cost reduction without the wind turbine. The main reason behind the result is the low average wind speed for the project selected location comparing with world average wind speed.

Table 11 Project cash flow summary

	Capital ($)	Replacement ($)	OMC ($)	Fuel ($)	Salvages ($)	Total ($)
PV	3,333	0	0	0	0	3,333
Diesel Generator	1,500	3,154	2,159	4,983	-367	11,430
Vision 6FM200D	1,250	3,923	1,147	0	-179	6,141
Convertor	1,000	417	1,147	0	-208	2,356
System	7,083	7,494	4,453	4,983	-754	23,261

In addition to the cost consideration, the hybrid system performance is examined in Figure 50, 51, 52, and 53 respectively. In Figure 50, the hybrid system electrical performance is examined with total PV generation of 46 % comparing with 54 % of diesel generation. Also, the total excess electricity per year is 376 kWh/year which represents about 5.38 % of the total generated power from the hybrid system.
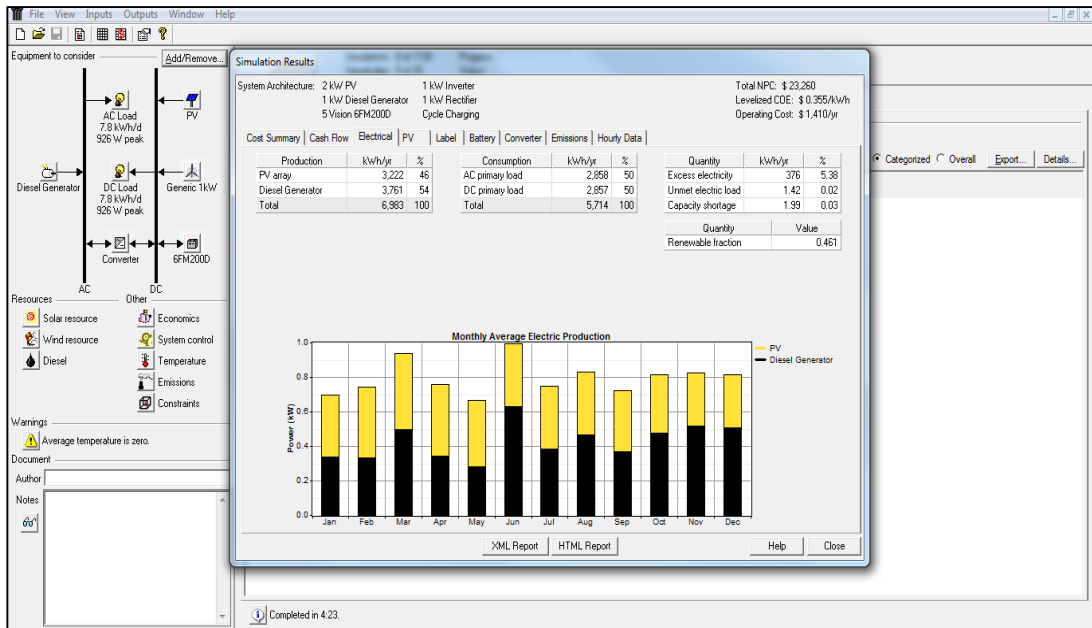
Figure 50 Hybrid system electrical performance

In Figure 51, the solar photovoltaic module performance is illustrated. With a rated capacity of 2 kW and mean output power of 8.83 kWh/day, the total PV production is 3222.95 kWh/year. Also, the total hours of operation is 4470 hours/year.

Figure 51 Solar photovoltaic module performance

In Figure 52, the yearly diesel generator performance is shown. With a 3756 hours of operation and total generated power of 3761 kWh/year, the diesel generator contributes with 54 % of the total power production of the hybrid power system. Moreover, the generator yearly fuel consumption is 1241 liters with a mean electrical efficiency of 30.8 %.
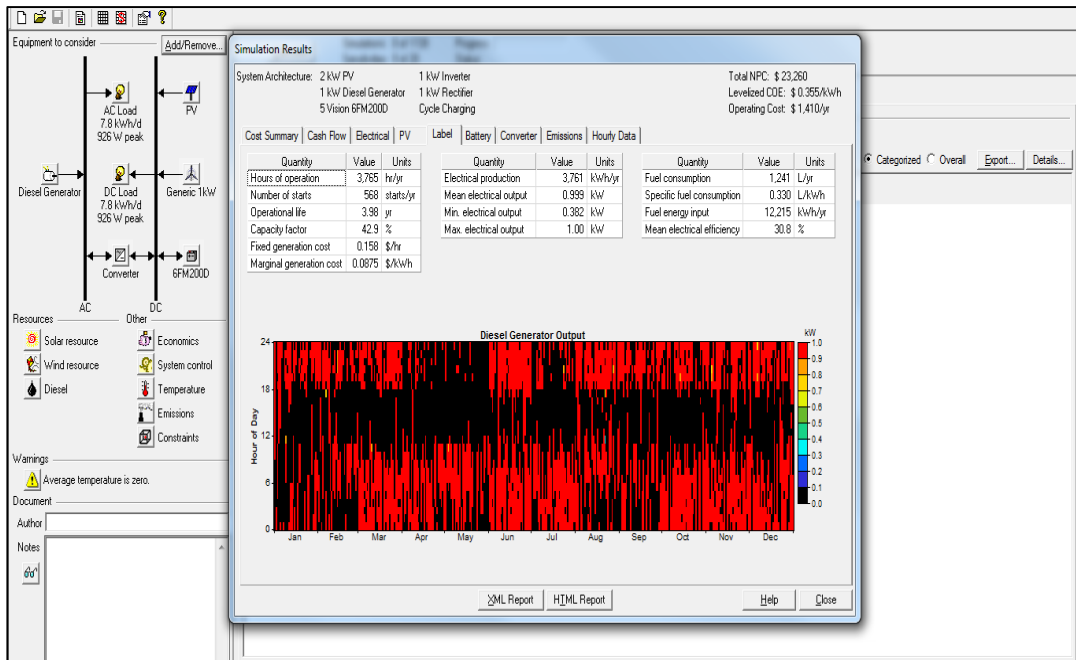
Figure 52 Diesel generator electrical performance
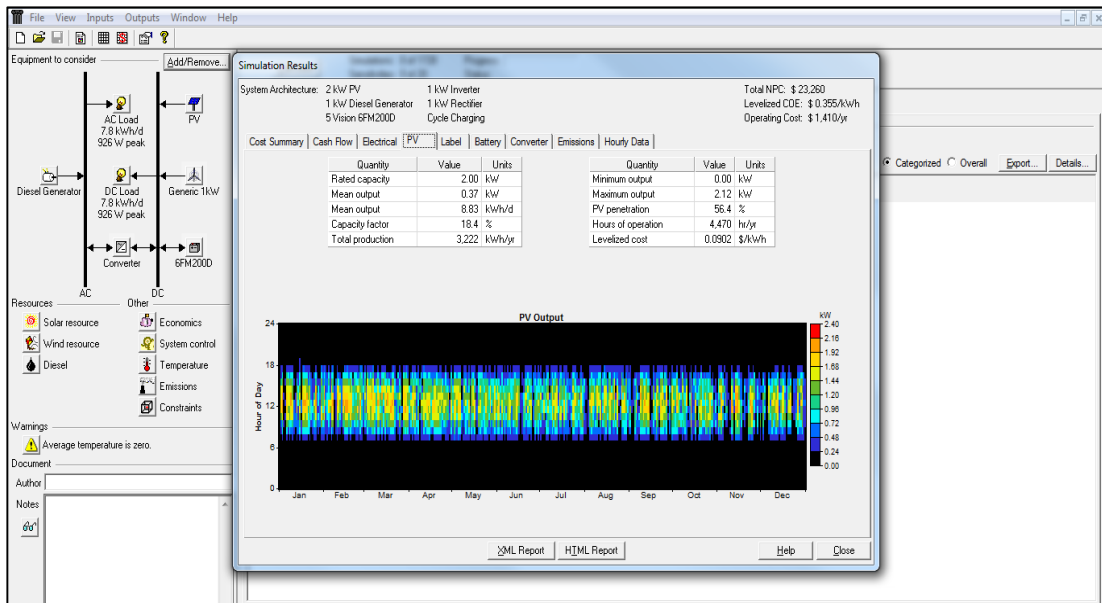
In Figure 53, the battery storage system performance is shown with detailed analysis of battery state of charge, battery lifetime and utilized battery bank size. The battery expected lifetime is 2.69 years with energy in and energy out of 1897 and 1523 kWh/year respectively. Furthermore, the average energy cost of the battery bank (5 batteries) is estimated to be 0.062 $/kWh.

Figure 53 Battery electrical performance

An additional study has been performed in the system along with the cost objective function which is the sensitivity study. The sensitivity study measures and analyzes

the effect of changing the values of system inputs on the optimum design components. For example, changing the average annual wind speed, changing the average annual solar irradiation level or changing the diesel price per liter. The project main objective was to achieve the lowest cost and it was mainly focused on the diesel price as an indicator to this objective.
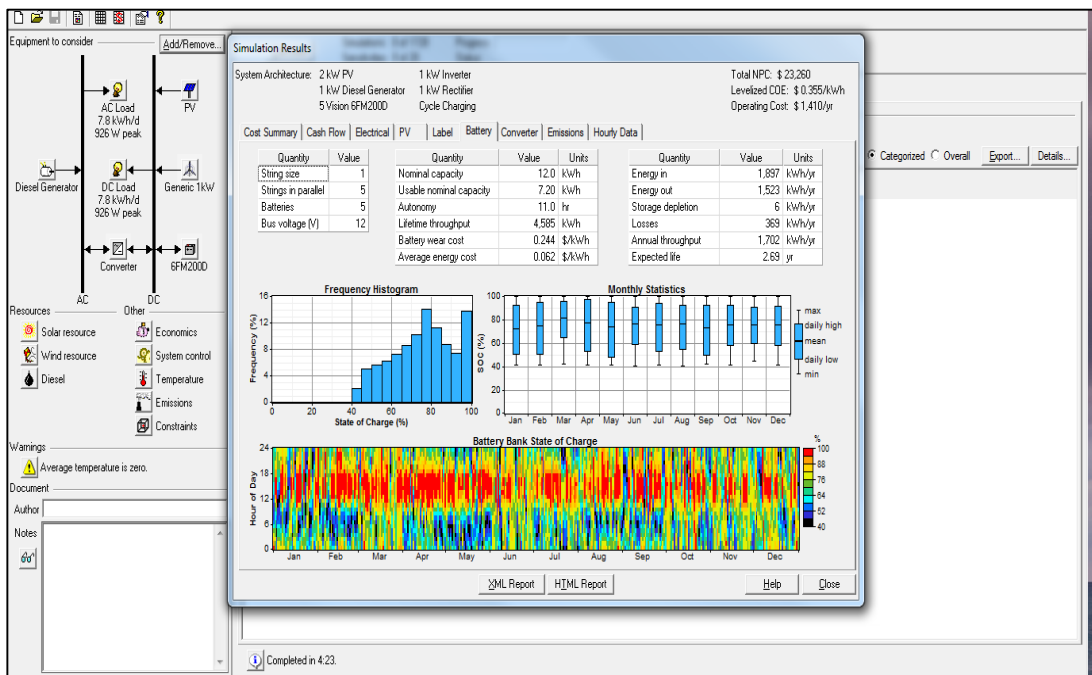
In the project, a sensitivity analysis was carried out on the hybrid system by varying the fuel price (diesel) per liter and running the optimization study for all the proposed values. Also, the sensitivity analysis had another variable to be considered during the simulation which is the changing in the nominal operating temperature of the solar photovoltaic modules. As it was discussed in the literature review of the project, the efficiency of the solar panel are greatly affected by the changing in the nominal operating temperature of the ambient environment. Hence, various operating temperatures were considered for the operation of the hybrid system. The effects of both sensitivity factor on the performance of the hybrid system are illustrated in Figures 54 and 55.
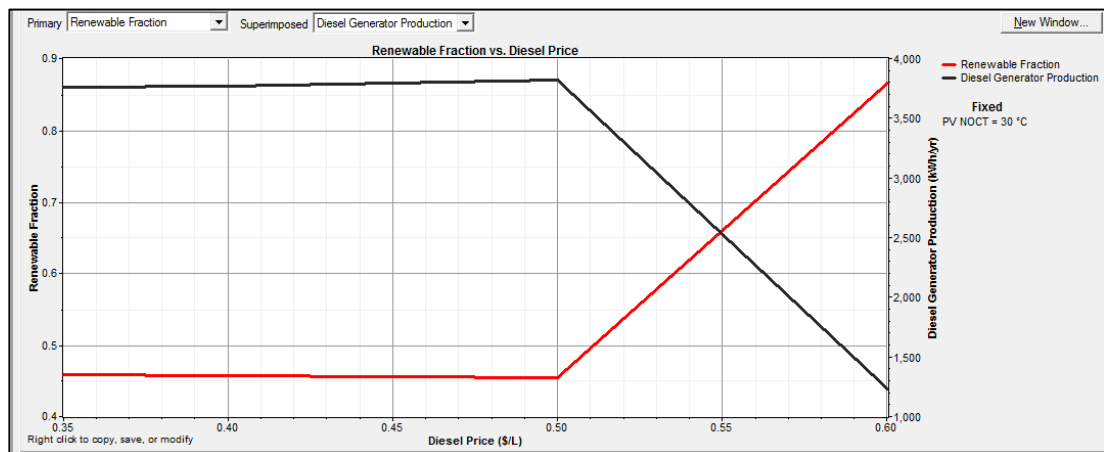
Figure 54 Renewable fraction vs Diesel generator production

In Figure 54, the solar photovoltaic total electrical production vs the diesel generator electrical production is examined. By using a sensitivity factor and varying the diesel price as well as the nominal operating temperatures for the solar panels, it can be seen that after a diesel price of 0.5 $/L, the value of the solar production will be increased and the value of the diesel production will be decreased. In other words, the optimum design of the hybrid system above 0.5 $/L for diesel price is aiming towards the renewable sources of energy which can maintain the system supply with the lowest cost.

However, by increasing the renewable energy production of the system, the capital cost will increase as a result of the commissioning and installation costs of new solar panels. On the contrary, the annual operation and maintenance cost of the hybrid system will be significantly decreased by implementing renewable sources as indicated in Figure 55.

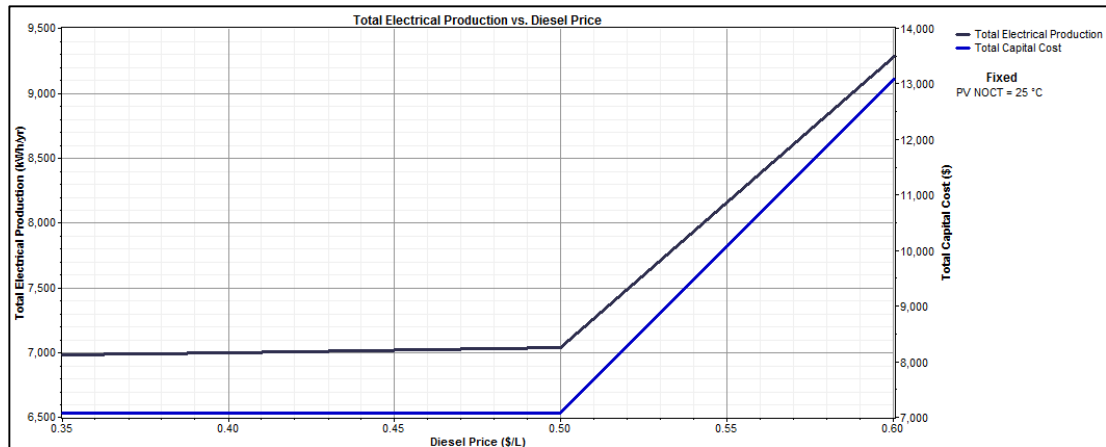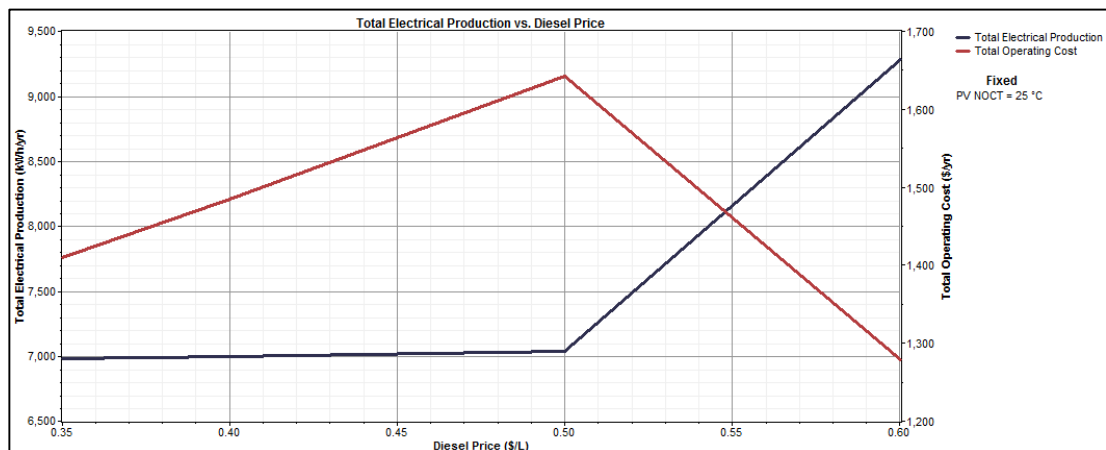Figure 55 Total capital cost of the system vs total electrical production

Figure 56 Annual operation and maintenance cost vs total production

In Figure 56, the annual operation and maintenance costs are significantly decreased after 0.5 $/L for the diesel price because the hybrid system will implement a more renewable sources approach which will decrease the fuel consumption and consequently the annual operating costs.

67

CHAPTER 5 : CONCLUSION AND RECOMMENDATIONS

Based on the project and its main objectives, a hybrid power system is suitable for installation and operation in the offshore environment of Malaysia. Moreover, the modelling study as well as the optimization study suggested that the hybrid system efficiency can be significantly increased by a proper and efficient utilization of the solar photovoltaic models in the system. Such an implementation would require a more efficient solar panels, a precise charging and converting control system and a well sized battery bank to preserve the excess generated power.

In addition to that, wind turbines utilization in Malaysia has proved to be less efficient than the solar photovoltaic models. As it was indicated in the literature review, the main reason for that is the low average wind speed in Malaysia comparing to other parts and countries in the world. However, by enhancing the control system of the implemented wind turbines, more energy can be harvested form the wind speed and hence a consistent, cheap and powerful supply of electricity could be ensured.

Furthermore, the diesel generator has proved to be a main backup for the hybrid system especially during the unfavorable climatic conditions which may affect the operation of wind turbines as well as solar photovoltaic panels. Also, the selection and sizing of the diesel generator, along with other hybrid system components, should be carried out after a detailed study about the offshore installation current load profile taking into considerations the future loads as well as the decreasing efficiency of the system while increasing the project lifetime.

Likewise, the optimization study has concluded that the fuel price of the diesel generator set will affect greatly the operation of the hybrid power system. By increasing the fuel price of the diesel generator, the dependence on the generator in supplying the offshore installations loads will be decreased. On the contrary, the renewable faction of the hybrid system will be increase by installing new solar panels or wind turbines which throughout the project life time will be much economically justified than using the diesel generator.

 Finally, the implementation of the proposed hybrid power system in the Malaysian offshore environment would have significant effects on offshore oil and gas operations. An effect which not only will be limited to the total reduction in costs but also reducing the emissions and preserve the environment.

REFERENCES

[1]   D. B. Evans and E. F. Yong, "Environmental Issues in Oil and Gas Development in Malaysia."

[2]   C. K. Seong and T. Y. Hong, "A Review Of Offshore Oil Fields Development In Malaysia."

[3]   C. C. Wan, "Use Of Unmanned Platforms In An Offshore Environment."

[4]   R. Rongsopa, "Hybrid Power Generation for Offshore Wellhead Platform: A Starting Point for Offshore Green Energy."

[5]   W. Zhou, "Simulation and optimum design of hybrid solar-wind and solar-wind-diesel power generation systems," 3313069 Ph.D., Hong Kong Polytechnic University (Hong Kong), Ann Arbor, 2008.

[6]   E. Lorenzo, "Solar Electricity Engineering of Photovoltaic Systems," *Artes Graficas Gala,* vol. S.L., 1994.

[7]   G. Walker, ""Evaluating MPPT converter topologies using a MATLAB PV model" " *Journal of Electrical & Electronics Engineering, Australia, IEAust,* vol.21, pp.49-56, 2001.

[8]   W. Schmitt, "Modeling and simulation of photovoltaic hybrid energy systems optimization of sizing and control," in *Photovoltaic Specialists Conference, 2002. Conference Record of the Twenty-Ninth IEEE*, 2002, pp. 1656-1659.

[9]   S. M. S., "Modeling and Simulation of Photovoltaic module using MATLAB/Simulink," *International Journal of Chemical and Environmental Engineering,* vol. Volume 2, 2011.

[10]   T. Ackermann, "Wind Power in Power Systems," *Wiley, England,* p. 1120, 2012.

[11]   H. F. Fujita, T Sekine, H. Senjyu, T. Sakamoto, R Urasaki, N. , "Output Power Levelling of Wind Turbine Generator for All Operating Regions by Pitch Angle Control. ," *IEEE Transactions on Energy Conversion,* vol. 21, pp. 467-475, 2006.

[12]   B. W. E. Association, "Environmental Impacts of Wind-Energy Projects," 2006.

[13]   M. M. Karrari, O. Rosehart, W., "Comprehensive Control Strategy for a Variable Speed Cage Machine Wind Generation Unit," *IEEE Transactions on Energy Conversion,* vol. 20, pp. 415-423, 2005.

[14]   P. V. B. Bongers, G. , "Wind turbine control design and implementation based on experimental models. ," *IEEE* vol. 2, pp. 2454-2459, 1992.

[15]   J. Martinez, "Modelling and Control of Wind Turbines," *Department of Chemical Engineering and Chemical Technology, Imperial College London,* 2007.

[16]   R. H. Harrison, E. Snel, H. , "Large Wind Turbines. ," *Wiley, England.,* 2000.

[17]   M. F. Balas, L. Johnson, K. Pao, L. , "Control of Variable-Speed Wind Turbines: standard and adaptive techniques for maximizing energy capture," *IEEE Control Systems Magazine,* vol. 26, pp. 70-81, 2006.

[18]   A. M. a. A. H. Al-Badi, ""Economics of wind turbine as an energy fuel saver a case study for remote application in oman"," *Energy,* vol. 34, pp. 1573-1578,2009.

[19] A. D. G. a. U. Hassan, ""what is power quality?," in Proceedings of the 10-th british Wind Energy Association Conference, D.J. Milborrow, London, March 1998, pp.22 24.

[20] M. d. r. n. d. Q. ebec, ""Strat´ egie´ energ´ etique," http://www. mrnf. gouv. qc. ca/energie/´strategie/ index.jsp, December 2011"

[21] R. N. B. S. A. Jalilvand, ""Design of a multilevel control strategy for integration of stand-alone wind/diesel system,"" *Interntional Journl of Electrical Power & Energy Systems,* vol. 35, pp. 123-137, February 2012.

[22] R. L. Lawrence, "Principles of Alternating Current Machinery ,2nd ed. The University of Michigan,Michigan : McGraw-Hili Book Company,Inc.,1920,2006"

[23] S. J. Chapman, "Electric Machinery Fundamentals, 5th ed. New York,USA: McGraw-Hili Companies,Incorporated,2011,2011"

[24] B. R. H. M. R. Jongerden, ""Battery Modeling," University of Twente, Twente,The Netherlands ,Technical Report 2012.

[25] I. R. JAOliver, JA. Cobos R.Prieto, ""Generic Battry Model based on a Paramaetric Implementation," Universidad Potecnica de Madrid 1 Centro de Electronica Industrial, Madrid, 2010"

[26] A. Y. Azman, A. A. Rahman, N. A. Bakar, F. Hanaffi, and A. Khamis, "Study of renewable energy potential in Malaysia," in *Clean Energy and Technology (CET), 2011 IEEE First Conference on*, 2011, pp. 170-176.

[27] K. S. e. aI, "Building Integrated Photovoltaic (BIPV) in Malaysia – Potential, Current Status Strategies For Long Term Cost Reduction," *ISESCO JOURNAL OF SCIENCE AND TECHNOLOGY,* vol. 1, 2005.

[28] M. Z. H. e. al., "Monitoring results of Malaysian Building Integrated PV Project in Grid-connected Photovoltaic system in Malaysia," *Energy and Power,* vol. 2, pp. 39 45, 2012.

[29] O. Authority for Electricity Regulation, "Study on Renewable Energy Resources," *Tech. Rep. 66847-1-1,* 12.05.2008.

[30] K. S. A. Baharuddin, C. H. Yen, S. Mat, and A. Zaharim, "Key success factors in implementing renewable energy programme in Malaysia," *WSEAS Transactions on Environment and Development, Algarve, Portugal,* vol. 4, pp. 1141- 1150, December 2008 [4th IASME/WSEAS International Conference on Energy, Environment, Ecosystems and Sustainable Development (EEESD'08) 2008.

[31] S. Mekhilef and D. Chandrasegaran, "Assessment of off-shore wind farms in Malaysia," in *TENCON 2011 - 2011 IEEE Region 10 Conference*, 2011, pp. 1351 1355.

[32] a. S. M. S. M. A. Elhadidy, "Parametric study of hybrid (wind+solar+diesel) power generating systems," *Renewable Energy,* vol. 21, pp. 129–139, October 2000 2000.

[33] F. Sulaiman, "Renewable energy and its future in Malaysia: a country paper," *[In: Proc. of Asia-Pacific Solar Experts Meeting, 1995],* 1995.

[34] Z. A. Z. E. P. Chiang, P. A. Aswatha Narayana, and K. N. Seetharamu, "The potential of wave and offshore wind energy in around the coastline of Malaysia that face the South China Sea," *International Symposillm on Renewable Energy: Environment*

Protection & Energy Soilltion for Sustainable Development, Kuala Lumpur, Malaysia, September 2003 2003.

[35]   P. B. Maria Kalogera, "Optimization of an Off-grid Hybrid System for Supplying Offshore Platforms in Arctic Climates," *The 2014 International Power Electronics Conference,* 2014.

[36]   M. a. S. Singh, S. , "Dynamic Models for Wind Turbines and Wind Power Plants," *National Renewable Energy Labratory,* 2011.